CHARACTERIZATION OF SENESCENT INTERVERTEBRAL DISC CELLS AND THEIR ROLE IN PERTURBATION OF MATRIX HOMEOSTASIS

by

Kevin Ngo

B.S., University of Pittsburgh, 2010

Submitted to the Graduate Faculty of

the Graduate School of Public Health in partial fulfillment

of the requirements for the degree of

Master of Science

University of Pittsburgh

2014

UNIVERSITY OF PITTSBURGH

GRADUATE SCHOOL OF PUBLIC HEALTH

This thesis was presented

by

Kevin Ngo

It was defended on

September 19, 2014

and approved by

Velpandi Ayyavoo, Professor, Department of Infectious Diseases and Microbiology

Graduate School of Public Health, University of Pittsburgh

David Rowe, Associate Professor, Department of Infectious Diseases and Microbiology

Graduate School of Public Health, University of Pittsburgh

Thesis Director: Nam Vo, Assistant Professor, Department of Orthopaedic Surgery

School of Medicine, University of Pittsburgh

Nam Vo, PhD

CHARACTERIZATION OF SENESCENT INTERVERTEBRAL DISC CELLS AND THEIR ROLE IN PERTURBATION OF MATRIX HOMEOSTASIS

Kevin Ngo, M.S.

University of Pittsburgh, 2014

ABSTRACT

Aging is the largest single risk factor for intervertebral disc degeneration (IDD). Dysregulated disc cells are thought to drive age-associated disc proteoglycan (PG) loss, a hallmark of IDD, through a combination of reduced capacity to synthesize matrix PG and increased production of proteolytic enzymes to breakdown matrix. The link between aged degenerative discs and cellular senescence has been previously observed in human discs, but it remains unknown if senescent disc cells are phenotypically different from their non-senescent counterpart in terms of matrix homeostasis. Hence, the goal of this study is to explore matrix homeostasis characteristics of senescent disc cells.

Outcome measures for anabolism have established that stress-induced senescence of human disc cells resulted in decreased PG synthesis, increased collagen type II expression in nucleus pulposus (hNP), and decreased collagen type I expression in annulus fibrosis (hAF). For catabolism, Western analysis revealed greater levels of ADAMTS- and MMP-generated proteolytic aggrecan fragments as a result of cleavage in the aggrecan interglobular domain (IGD) in the conditioned media (CM) of H_2O_2–induced senescent hNP cells compared to control. In contrast, the levels of aggrecan IGD proteolytic fragments were relatively unchanged in the CM of senescent hAF cell culture compared to non-senescent hAF cell culture. ELISA and antibody array experiment showed elevated levels of many pro-inflammatory cytokines (IL-6, IL-8, PDGF-BB, GCSF), chemokines (EOTAXIN-2, IP-10, RANTES) and MMPs (MMP-1,

MMP-3, MMP-10) in the CM of senescent hNP cells. These are key factors previously reported for senescence-associated secretory phenotype (SASP) of stress-induced senescent cells which impart profound catabolic effects on neighboring cells and the extracellular matrix. The total GAG content moderately decreased in senescent hAF and significantly decreased in senescent hNP cell cultures compared to non-senescent cell culture control.

These *in vitro* findings suggest that senescent disc cells perturb extracellular matrix homeostasis via acquisition of SASP, reduced matrix synthesis capacity, and increased matrix degradation. Identifying and confirming cellular senescence as a driver of disc PG loss and IDD will offer novel opportunities for targeted therapy to prevent or treat IDD, which would have a tremendous public health impact in preventing or ameliorating chronic low back pain.

TABLE OF CONTENTS

LIST OF TABLES

LIST OF FIGURES

PREFACE

I would like to thank my advisor and mentor Dr. Nam Vo for the opportunity to initially volunteer as an undergrad in the Ferguson Laboratory for Orthopaedic and Spine Research. It was a great opportunity for me to gradually gain skills and experience. Through this initial opportunity, I was able to meet one of the most diverse groups of students, residents, fellows, and mentors. Without this opportunity, I would not have been able to attend graduate school and expand my skills and knowledge while gaining invaluable scientific and interpersonal experience.

I will be forever grateful to the Ferguson Laboratory for Orthopaedic and Spine Research. I would like to extend my eternal gratitude to Dr. James Kang and Dr. Gwen Sowa for the guidance, constructive feedback, and being such great role models in both professional and personal life. Also, I'd like to thank Mary Lou Duerring and Lori Freund for always taking care of business literally and interesting conversations. I'd like to also thank Dr. Kevin Bell and Dr. Rob Hartman for the research guidance, friendship, and willingness to help with any issue as well as some of the most interesting conversations. To the almost always impressive group of international fellows, I thank Drs. Takashi Yurube, Luigi Nasto, Hong Joo Moon, and Pedro Pohl for their sharing the skills, experience, and knowledge with me in research and in personal life. I would also like to express my thanks to Joao Paulo Coelho and Dr. Douglas Bentley for

research/personal guidance and friendship as well as the absolute best conversations. I'd like to thank to Dr. David Phillibert and Nora Sherry for the opportunity to work together, fun conversations, and friendship. I also thank Dr. Wan Huang and Qing Dong, for their patience, teaching, and never dull conversations.

I'd like to extend gratitude towards the medical residents I've had the pleasure of working with and getting to know: Drs. Lloydine Jacobs, Michael McClincy, Tiffany Kadow, and Karl Henrikson. Also for Joao Paulo Coelho and Dr. Mike McClincy, thanks for the inspiration to get fit with exercise and diet. Also, I'm extremely grateful for the opportunity to work with and get to know many medical students over the years with diverse skill set and backgrounds. Overall, the cumulative experience of my 6 years in the lab (so far) has led me to pursue admission to medical school after finishing graduate school. I'd like to truly express eternal gratitude again to Dr. Nam Vo for his patience, giving me an employment opportunity, always interesting conversations about science and everything else, and friendship.

I'd like to thank the faculty and staff of IDM for all the teaching and advising over the last two years including Dr. Ayyavoo and Dr. Rowe for serving on my committee and providing valuable insight and constructive criticisms and Dr. Reinhart for serving as my IDM advisor. I extend my gratitude to the friends I've made in IDM: Suha Abdelbaqi, Fortuna Arumemi, Aiymkul Ashimkhanova, Lyndsay Avery, Jessica Battaglia, Jessi Bond, Andrea Dobbs, Parichat "Amp" Duangkhae, Nicholas Giaccobi, Mary Hasek, Nicole Phillips, Benjamin Policicchio, and Jennifer Stock for making the journey of graduate school easier and a lot more fun. I have no doubts about the success each of you will have in your future careers.

The following may not seem like a serious expression of gratitude, but it is. I seriously thank Paramore and Taylor Swift for inspiring me and creating music that has led me through countless hours of writing, studying, pipetting, commuting, and "dancing". Now back to people I personally know: I'd like to thank my best friends Bryan Behr and Regina Caldart for being supportive, the conversations and time spent together, and ultimately for their friendship. Lastly, I owe my life to my parents, David Ngo and Na Ly, for raising me and providing the opportunities to succeed. Also thanks for spending a substantial portion of your earnings and time on me and having ultimate patience with me over the years. I strive to eventually pay them back at least in part for all they've sacrificed for me in the coming decades.

1.0   INTRODUCTION

1.1   INTERVERTEBRAL DISC DEGENERATION (IDD)

1.1.1   Disc Biology

The intervertebral disc (IVD) is a fibrocartilaginous structure (Figure 1) surrounded by longitudinal ligaments laterally and vertebrae axially. The IVD is sandwiched between cartilage endplates (CEPs), which contain the ends of capillaries from the vertebral vascular network important for delivering nutrients to the disc [1, 2]. Disc annulus fibrosis (AF) consists of mostly collagen type I fibers surrounding the proteoglycan-rich gelatinous nucleus pulposus (NP). The NP contains randomly organized collagen type II fibers, elastin fibers, with sparsely interspersed notochordal and chondrocyte-like cells [3, 4]. The AF consists of 15-25 concentric rings (lamellae) with 60-degrees-to-vertical positioned parallel collagen fibers. Embedded within each ring are elongated, fibroblast-like cells positioned parallel to the collagen fibers [3, 5].

During the transition from outer AF to inner AF and NP, there is less collagen type I and more collagen type II [6, 7]. Mechanically, the AF acts to withstand the tensile strain while the NP counteracts compressive force in the spine [8, 9]. Thus IVDs serve to bear load and provide flexibility to the spine.

1

The high proteoglycan (PG) content in the NP attracts counterions from the negatively charged sulfates on the chondroitin- and keratan-sulfate glycosaminoglycan (GAG) sidechains on PG (Figure 1), generating high osmotic gradient and imbibing a large amount of water, which enables to the NP to resist compression. Matrix homeostasis, a proper balance of matrix catabolism and anabolism, is essential for the functional health of the disc. Disc matrix catabolism involves the breakdown of the extracellular matrix typically mediated by A Disintegrin And Metalloproteinase with Thrombospondin Motifs (ADAMTSs), and Matrix Metalloproteinases (MMPs). Disc matrix anabolism is determined principally by synthesis of the two major classes of disc structural matrix constituents, collagens, and proteoglycans (Figure 2). The main proteoglycan in disc NP tissue is aggrecan.

Development and remodeling of the disc depend on the disc cells' ability to synthesize new matrix and degrade existing matrix by secreting proteases (ADAMTSs and MMPs), the products of which can be detected with molecular markers (more abundant during development before adulthood) [8, 10-17]. During transition to adulthood, the NP composition undergoes changes, including an increase in collagen content resulting in a texture and consistency change from translucent liquid to soft, gelatinous tissue.

The NP contains the maximum PG amount during the young adult phase, followed by progressive PG decline with age [8]. This remodeling process during development may contribute to the varied compressive loads that adult discs can handle (between 2.8 and 13.0 kiloNewtons (kN)) [8, 18].
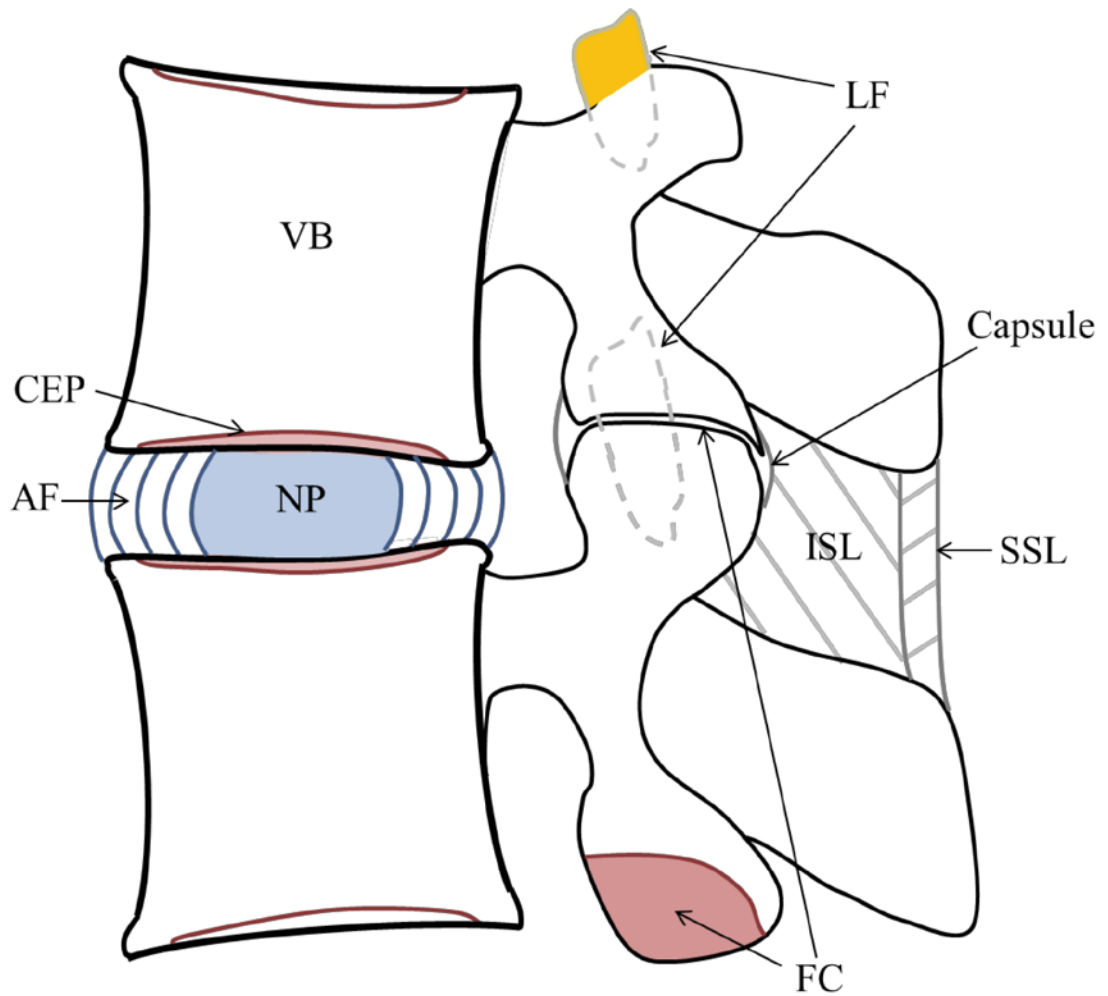
This sketch represents the anatomy of the intervertebral disc (IVD) and surrounding structures. A functional spinal unit (FSU) consists of vertebrae, IVD, facet joints, and ligaments. ISL and SSL: Interspinous and Supraspinous Ligaments, which are posteriorly positioned between the spinous processes (function to protect nerves). FC: Facet Cartilage (composed of hyaline cartilage) makes up facet joints along with joint capsule, synovium, and synovium fluid. CEP: Cartilage Endplate connects the IVD to vertebral body. NP: Nucleus Pulposus (gelatinous center of the IVD surrounded by AF). AF: Annulus Fibrosis (outside NP-surrounding structure of the IVD). Adopted with permission from Dr. Robert Hartman.
Figure 1. Structural components and organization of the intervertebral disc and functional spinal unit.
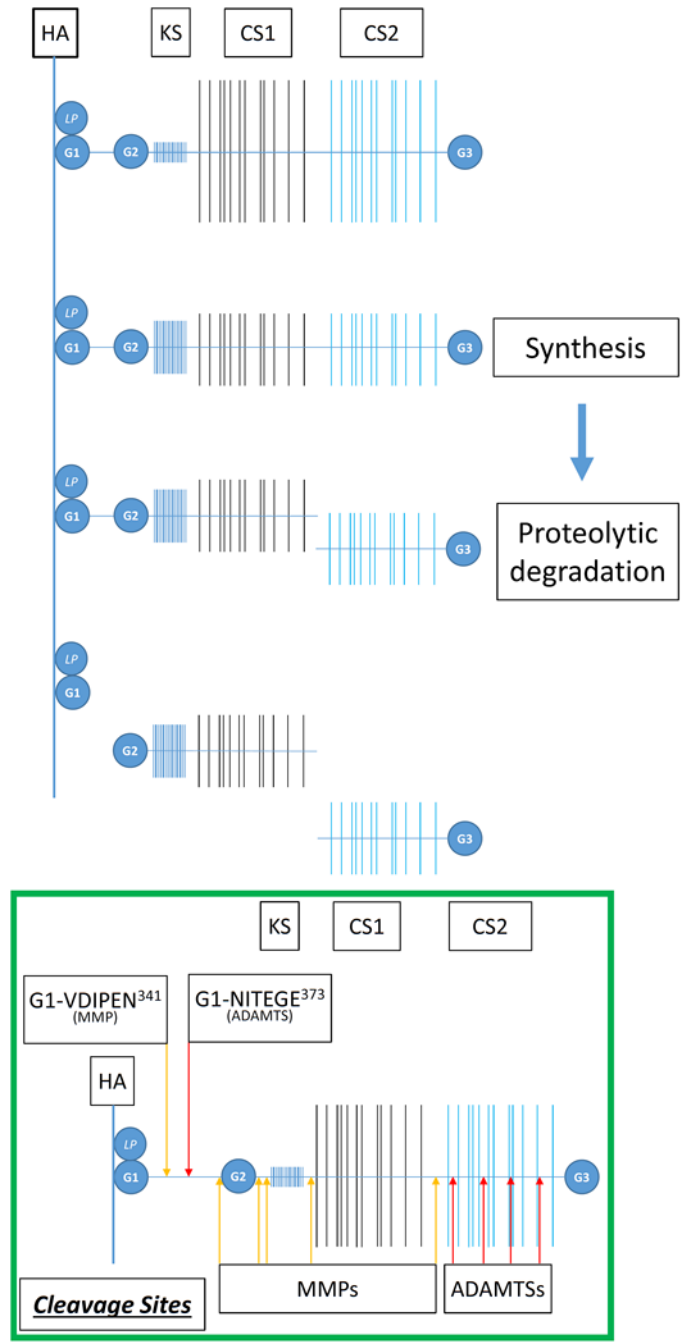
The components of a disc proteoglycan aggregate include proteoglycan, hyaluronic acid (HA), and link protein (LP). Proteoglycan binds noncovalently to HA, and this interaction is mediated by LP. A disc proteoglycan unit consists of the core protein aggrecan to which glycosaminoglycans such as chondroitin sulfate and keratan sulfate are covalently attached. G1, G2, G3 are globular, folded regions of the central core protein aggrecan [9]. Known cleavage sites of proteases ADAMTSs and MMPs on aggrecan [19, 20]. CS1 and CS2: Chondroitin Sulfate attachment domains 1 and 2. KS: Keratan Sulfate. LP: Link Protein.

Figure 2. Structural components and organization of aggrecan.

1.1.2 IDD Features

Intervertebral disc degeneration (IDD) has been defined as the abnormal, cell-mediated process of progressive loss of PG matrix and eventual failure of the disc structural integrity [8]. IDD leads to many biochemical and mechanical changes in the IVD, which interferes with the natural function of the spine. Early characteristics of IDD include loss of PG and water content of the NP due to matrix homeostatic imbalance. Late stage macroscopic changes associated with IDD include annular fissure, collapse of disc height, and formation of neo-osteophytes in the adjacent cartilaginous endplate and vertebrae. IDD is associated to pathological conditions such as disc herniation, low back pain, and spinal stenosis (narrowing of the spinal canal leading to pressure on the spinal cord). There are many influencing factors involved in IDD, including genetic predisposition, impaired nutrient supply, changed enzyme activity level, cellular senescence and apoptosis, changes in matrix and water content, failure of structural integrity, and neurovascular ingrowth [8, 21].

1.1.3 Current IDD Therapies

Many patients with IDD and LBP have resolution of their pain with conservative treatments such as medications (nonsteroidal anti-inflammatory drugs (NSAIDs), acetaminophen, muscle relaxants [22-24]) and physical therapy [22, 25, 26]. The traditional, archaic prescription of bed rest has actually shown to be less effective than physical activity for recovery due to muscle deconditioning [22, 27]. If conservative treatments fail after 6 to 12 weeks [22, 28], current

medical interventions for IDD mainly are surgeries with the goals of removing potential pain generating sources and restoring natural supportive disc functions for everyday motions.

Current biologic strategies for IVD regeneration have been focused on mainly cell-based approaches with and without tissue-engineered scaffold. The primary goal of these therapies is to increase the net ECM content in the disc. There has been less of an emphasis of the effect of these therapies on potentially depleting the disc nutrient supply, which is thought to drive IDD [2, 8]. The IVD is the largest avascular tissue in the body which creates a hypoxic environment with decreasing oxygen concentration gradient from the outer AF to the inner NP [29]. Nutrient supply to the NP cells specifically is quite limited due to the lack of a vascular supply with the capillaries ends reaching to only the CEP. The balance of anabolism and catabolism by the IVD cell population is maintained in a healthy disc, however during IDD, degradation may overtake synthesis of ECM components causing a net loss of matrix and thus drives disc degeneration [30].

A potential harmful effect of cell-based therapies is the introduction of additional demand on the limited level of nutrients in native discs with the newly introduced mesenchymal stem cells (MSCs) without increasing the supply of nutrients [2], which may limit long term effectiveness of such therapies due to nutrient starvation. In degenerated discs, the chronic state of inflammation may increase the glucose consumption and lactic acid production rates resulting in an increased cellular nutrient demand with reduced supply (transport rate) into the degenerated disc [2, 31, 32].

Therefore, this evidence points towards an overall reduced nutrient availability for the disc cells either due to reduced transport rate of nutrients or increased cellular demand. Thus, cell-based therapies to treat IDD have to take into consideration the disc limited nutrient environment.

1.2   LOW BACK PAIN AND IDD

Low back pain (LBP) is the second leading cause for a patient consulting a physician in the US, just behind upper respiratory infections [33]. About 80% of the US population will experience back pain during their lifetime [34] while greater than 25% of Americans experience LBP annually [35]. These LBP patients experience a drastic decrease in the quality of life due to chronic pain and restricted mobility. With LBP, there is a large economic burden from the socioeconomic cost of the direct medical costs (and non-health care associated costs – food, travel, etc.) as well as the indirect costs due to reduction of employment and household productivity. The total of these socioeconomic costs exceeds $100 billion in the US [36]. Intervertebral disc degeneration (IDD) is the leading underlying causative factor of LBP.

1.3 AGING AND IDD

1.3.1 Aging Drives IDD

There are several proposed causes of IDD, including genetic predisposition, overloading-induced injury of the IVD, smoking, and aging. Of these, aging is the biggest etiologic factor because disc matrix PG is invariably and progressively lost with age [37, 38]. How aging disrupts disc matrix homeostasis leading to PG loss and IDD is not clearly understood. Hence, understanding the biology of disc aging is critical in developing effective therapeutic interventions to delay and or treat age-related IDD disorders. This is imperative because of the growing aging population which is expected to bring great burdens and challenges from the many age-related diseases. By 2050, the world population is predicted to be comprised of 1.5 billion of ages 65 and older compared to 524 million in 2010 [39, 40].

1.4 CELLULAR SENESCENCE AND AGING

1.4.1 History of Cellular Senescence

The biological purpose for senescence has been thought to be similar to apoptosis, which is to prevent the proliferation of or eliminate undesired, damaged cells that are now harmful to the host [41]. Senescent cells are the opposite of cancer cells in terms of their respective proliferative properties. The activation of cyclin-dependent kinase (CDK) inhibitors p16, p15, p21, p27 is the converging point of all senescence-inducing stimuli, which ultimately resulting in hypo-

phosphorylation of retinoblastoma (RB) and termination of proliferation [41-46]. After experiencing stressful stimuli, the cell decides whether to attempt self-repair to continue dividing or undergo senescence to stop dividing as a mechanism of preventing tumor formation from accumulated cellular damage. Senescence is initiated acutely with the likes of IL-1α followed by the establishment of the Senescence-Associated Secretory Phenotype (SASP) with the secretion of cytokines and chemokines, which recruit immune cells with the purpose of clearance of the damaged cell [47]. However, it is proposed that the rate of immune clearance of senescent cells is eventually outpaced by the accumulation of senescent cells with age. This occurs even with the potential attenuation of SASP with microRNAs such as mir-146a and mir-146b, which drives aging in cells, tissues, and ultimately the host [47, 48].

1.4.2 Cellular Senescence as a driver of Aging

Senescence was initially discovered by Leonard Hayflick and Paul Moorhead who observed that human fibroblasts have a limit on their proliferative capacity, and subsequent studies associated cessation of cell proliferation with telomere shortening [41]. Such replicative cell senescence was then thought to be a protective mechanism against tumorigenesis. However growing evidence now suggests that cellular senescence as a key driver of organismal aging. Senescent cells have been found to be increased in aged and diseased tissues in age-associated comorbidities such as Alzheimer's disease [49, 50], Parkinson's disease [51], glaucoma [52], atherosclerosis [53, 54], COPD [55-58], osteoarthritis [59-62], Type 2 diabetes [63, 64], and cancer [65, 66] in elderly. Stress-induced senescent cells have been shown to acquire senescence-associated secretory phenotype (SASP) which result in the increased production and secretion of pro-inflammatory cytokines, chemokines, growth factors, and matrix

9

metalloproteinases (MMPs) including IL-6, IL-8, MMP1, and MMP3 [67]. Importantly, clearance of senescent cells is reported to delay age-associated disorders in a progeroid mouse model [68-71]. Therefore, elucidating mechanisms of senescence may provide new therapeutic strategies to delay age-associated comorbidities, which would have a profound public health impact by attacking many chronic diseases early on by limiting the most critical risk factor of aging.

1.4.3 Therapeutic Strategies to eliminate Cellular Senescence

Two possible therapeutic strategies for targeting senescence are interfering with signaling pathways that result in senescence-associated cell cycle arrest and targeting SASP to minimize harmful effects [40]. Inhibiting proliferation arrest via interfering with the signaling pathways (p16, Rb, p53) may have unintended effects such as the loss of tumor surveillance mechanisms for preventing cancer. Prevention of the chronic development of SASP may provide a balance of senescence with preservation of its four functions of tumor suppression, tumor promotion, aging, and tissue repair while limiting the "harmful" functions [47].

Another therapeutic strategy for many chronic diseases is the targeted removal of senescent cells, themselves are the underlying source of chronic state of inflammation, with the goal of restoring function to tissues [68]. Of course, the caveat would be identifying a specific marker of senescent cells to selectively target them for removal. Those individuals living to 100 years of age or older (centenarians) have been observed to have low levels of senescent CD8$^+$ CD28$^-$ T cells that may indicate preserved immune function [72, 73].

Thus the removal of senescent cells may enhance the innate and adaptive immune responses of the elderly extending lifespan while improving quality of life (via restoring some tissue functionality) leading to reduced socioeconomic burden via limiting tertiary prevention healthcare costs [68].

1.4.4 Cellular Senescence in Disc

Cellular senescence has been previously noted as accelerated in aged, degenerated discs compared to healthy discs both in humans and animals [74, 75]. These senescent cells have also been associated with increased catabolism, which supports the hypothesis that cellular senescence is a potential driver of IDD. The percentage of senescent and proliferating cells has been compared in human AF *in vivo* with the observations of increased senescent cells in degenerated discs compared to control discs [75] and low cell proliferation in both young and degenerated discs. However, whether senescent disc cells are a causative driver of age-related IDD and how they do so are important questions which have not been addressed.

2.0   OBJECTIVE

2.1   HYPOTHESIS

Aging is the largest risk factor for IDD, which is a condition that contributes to many debilitating spinal disorders and disabilities with a tremendous socioeconomic burden [76]. Loss of disc matrix proteoglycan (PG) is a hallmark of age-related IDD as a consequence of perturbed matrix homeostasis, a combination of cell-mediated changes in PG synthesis (decreased) and PG proteolysis (increased) [1]. Although elevated levels of senescent disc cells have been linked to IDD in aged discs, the phenotype and characteristics of senescent disc cells have not been explored. Based on the reported findings in the literature, I hypothesized that senescent disc cells acquire imbalanced matrix homeostasis which drives age-related loss of matrix PG leading to IDD. I propose to test this central hypothesis with the following specific aims.

2.2   SPECIFIC AIMS

Aim 1: **To test the hypothesis that senescent human disc cells perturbs matrix homeostasis by decreasing the anabolism of the disc matrix.**

Aim 2: **To test the hypothesis that senescent human disc cells perturbs matrix homeostasis by increasing the catabolism of the disc matrix.**

<u>Approach.</u>

<u>Induction and confirmation of senescence.</u> Human disc cells isolated from surgical specimens were exposed to hydrogen peroxide treatment twice using the previously established oxidative induction of senescence method treatment [77]. Senescence phenotype was verified by assaying for the SASP, senescence-associated β-galactosidase (SA β-gal) staining for SA β-gal activity, brightfield microscopy for cell morphology, trypan blue exclusion assay for cell proliferation.

<u>Matrix Anabolism.</u> To assess matrix anabolism, the oxidative stress-induced senescent human NP and AF cells were measured for their total glycosaminoglycan (GAG) content by the DMMB colorimetric assay and normalized to total cell number or DNA amount by Picogreen assay. Quantitative RT-PCR was performed to assess the relative gene expression of matrix structural components: Aggrecan, Collagen 1, Collagen 2, Versican, and Link Protein.

<u>Matrix Catabolism.</u> Western blotting was performed to assess the ADAMTS- and MMP-generated catabolic degradation of aggrecan proteins. SASP profile was determined using inflammation and MMP antibody arrays (40 targets and 10 targets, respectively) to assess levels of other inflammatory proteins that senescent hNP or hAF cell may produce and secrete. To assess the active state of secreted MMPs, MMP enzymatic activity from the conditioned media was measured.

3.0   MATERIALS AND METHODS
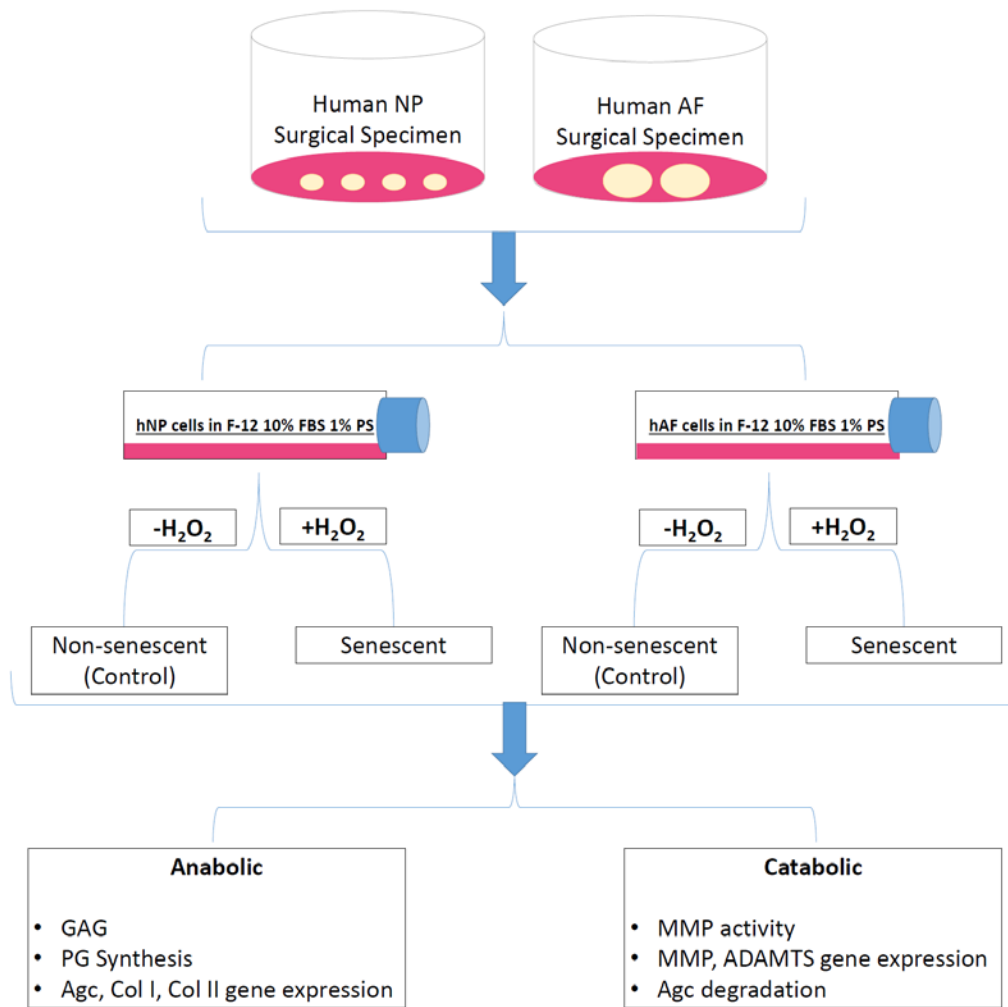
Figure 3. Overall experimental design

3.1 SAMPLE COLLECTION AND CELL ISOLATION

Human AF and NP samples were obtained from surgical specimens (Table 1) from generally older 47.7 ± 11.4 years (mean ± SD) patients with diagnoses of stenosis or herniated disc generally (Figures 3 and 4). These tissue samples were washed, minced, and digested in 0.2% pronase (*EMD Chemicals* 53702) for one hour then 0.02% collagenase P (*Roche Applied Science* 11213873001) overnight. The following day these cells were filtered and then plated onto tissue culture-treated flasks.

Table 1. De-identified patient information

Age	Sex	Diagnosis	Disc Level	Degen. Grade	Smoker	Diab-etic	Outcome Measures
56	M	Cervical Stenosis	C5-6, C6-7	2	Yes	N/A	ELISA
59	F	Cervical Stenosis	C3-4, C4-5	3	Yes	N/A	ELISA
49	M	Cervical Stenosis	C5-6, C6-7	3	Yes	N/A	ELISA
44	M	Cervical Disc displacement	C5-6, C6-7	2	No	N/A	ELISA
40	F	Herniated Disc	C6-7	2	Yes	N/A	Ab Arrays
48	F	Herniated Disc	C5-6, C6-7	2	Yes	N/A	PCR Catabolic
68	F	Cervical Stenosis	C6-7	3	No	N/A	PCR Catabolic
53	F	Cervical Stenosis	C4-5, C5-6	2	No	N/A	PCR Catabolic
33	F	Cervical Stenosis	C5-6, C6-7	3	Yes	N/A	Ab Arrays
56	M	Cervical Stenosis	C3-4, C4-5	2	Yes	N/A	PG Synthesis
48	M	Cervical Stenosis	C5-6, C6-7	3	Yes	N/A	PG Synthesis
60	F	Scoliosis	L5-S1	3	Yes	N/A	PG Synthesis
46	F	Cervical Stenosis	C4-5, C5-6	Unknown	Yes	N/A	Ab Arrays

Table 1. Continued

32	F	Non-Union	L4-5	2	Yes	N/A	Ab Arrays
38	M	Cervical Stenosis	C5-6, C6-7	2	N/A	N/A	PCR Catabolic
45	F	Cervical Stenosis	C4-C7	2	No	N/A	PCR Anabolic, PCR Catabolic
54	F	spondylotic stenosis	C5-C6, C6-C7	2	No	No	PCR Anabolic, PCR Catabolic
56	M	spondylotic stenosis	C5-C6, C6-C7	2	No	No	PCR Anabolic, PCR Catabolic
55	F	cervical stenosis and radiculopathy	C5-C6, C6-C7	3	No	No	PCR Catabolic
28	F	lumbar stenosis	L4-L5, L5-S1	2	No	No	PCR Anabolic
52	M	herniated disc	C4-C6	3	No	No	PCR Anabolic, GAG, Western
21	M	cervical stenosis	C3-C4, C4-C5	2	No	No	PCR Anabolic, GAG, Western
57	F	cervical stenosis	C5-C7	3	No	No	GAG, Western
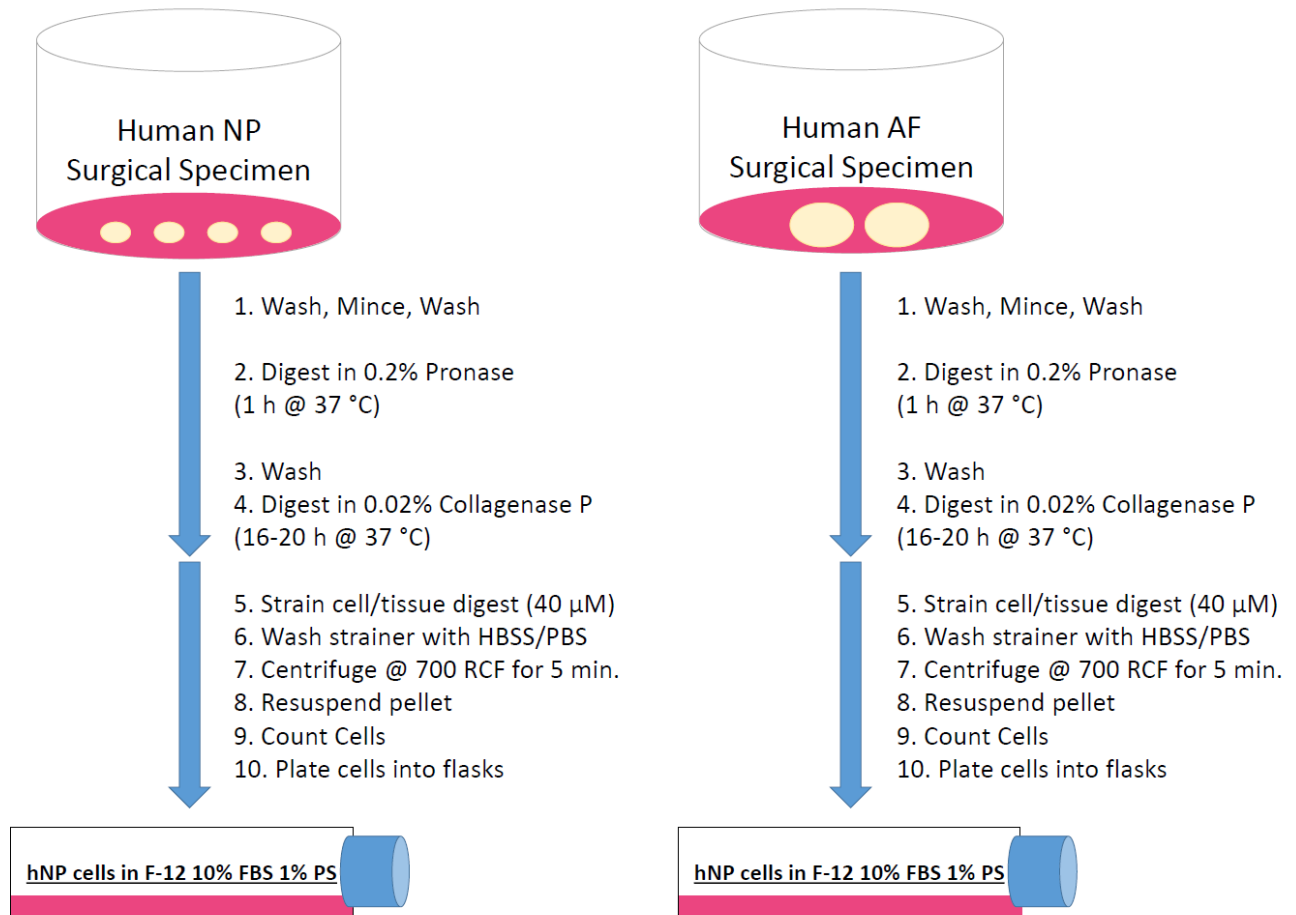
Figure 4. Detailed experimental protocol for tissue processing and disc cell isolation

3.2   INDUCTION AND CONFIRMATION OF CELLULAR SENESCENCE

To induce cellular senescence and SASP (Figure 5) by oxidative stress, we used the previously established hydrogen peroxide treatment at normoxic culture conditions (atmospheric 20% O_2) [77]. Greater number of cells (two fold that of untreated control: 50,000 cells (Figure 5)) were treated with 500 µM hydrogen peroxide in F-12 10% FBS 1% PS for two hours then changed to regular media F-12 10% FBS 1% PS (*Life Technologies* 11765-062, *Atlanta Biologicals* S12450, *Life Technologies* 15140-16), split onto new plates and incubated overnight at 37°C and normoxic culture conditions, treated again with 500 µM hydrogen peroxide in F-12 10% FBS 1% PS for two hours (*Life Technologies* 25300-120), changed to fresh regular media F-12 10% FBS 1% PS, and incubated at 37°C and normoxic culture conditions for 4 days followed by sample collection to allow enough time for the development of SASP (Figure 5).

Senescence-associated β-galactosidase (SA β-gal) staining [78] was done after the above treatment in 12 well plates by washing the cells with PBS then fixing with 2% paraformaldehyde (*Sigma-Aldrich* P6148) and 0.2% gluteraldehyde (*Sigma-Aldrich* G5882) for 5 minutes. This was followed by a PBS wash and overnight incubation with a staining solution: 40 µL 1M Magnesium Chloride (*Sigma-Aldrich* M8266), 600 µL 5M Sodium Chloride (*Sigma-Aldrich* S3014), 2 mL100mM Potassium Ferrocyanide (*Sigma-Aldrich* P3289), 1 mL 20 mg/mL X-gal (*Sigma-Aldrich* B4252) in dimethylformamide (*Sigma-Aldrich* D4551), 4 mL 0.2M Citric Acid/Dibasic Sodium Phosphate Buffer (*Sigma-Aldrich* 251275), 12.4 mL Water). Images were taken using brightfield microscopy at 40X magnification.
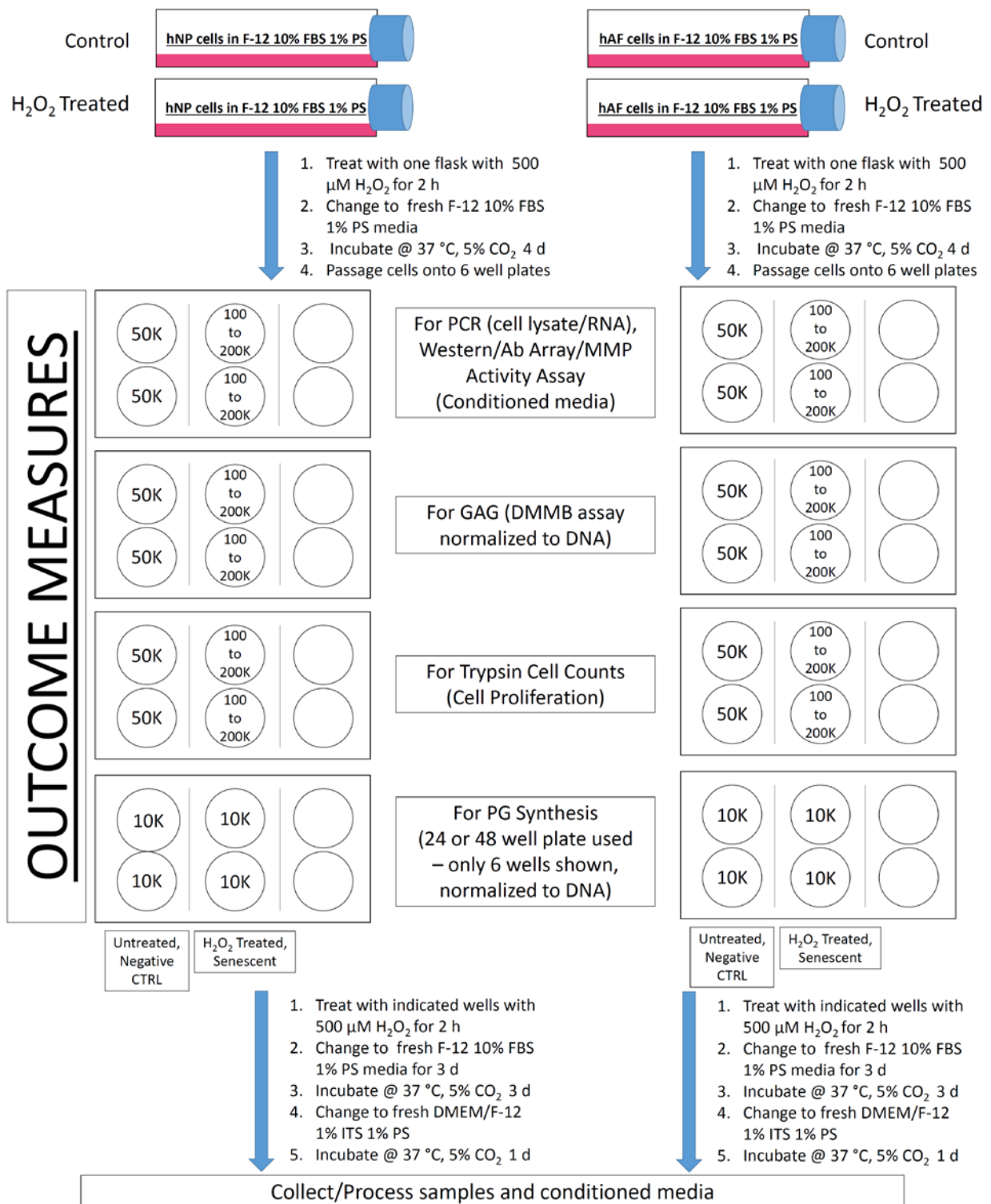
Figure 5. Detailed experimental protocol for cell culture, treatment with hydrogen peroxide, and sample collection for different outcome measures.

3.3   MATRIX ANABOLISM: PROTEOGLYCAN SYNTHESIS AND GENE EXPRESSION

To characterize PG metabolism, PG synthesis was measured by ^{35}S-sulfate (*American Radiolabeled Chemical* ARS-105) incorporation by adding radiolabeled media to the cells for 2 to 3 days followed by adding homogenization buffer containing 200 mM Sodium Chloride, 50 mM Sodium Acetate, 0.1% Triton X-100 (*Sigma-Aldrich* X-100), 10mM EDTA, 50 µM DTT (*Sigma-Aldrich* D9779), and 1x Protease Inhibitor (*Sigma-Aldrich* P8340) to each well at 4 °C for 1 hours with shaking. Next, in a separate 1.5 mL microcentrifuge tube, the homogenization buffer is then added to a Guanidine Hydrochloride extraction buffer containing 8M Guanidine Hydrochloride (*Sigma-Aldrich* G3272), 50mM Sodium Acetate, 10mM EDTA, and 1x Protease Inhibitor at 4 °C for 4 hours with shaking to extract proteoglycans [79]. The processed samples in homogenization and GHCl were mixed with Alcian Blue solution containing 0.02% Alcian Blue (*Sigma-Aldrich* A9186), 50mM Sodium Acetate, and 85mM Magnesium Chloride. for an hour at room temperature then loaded onto nitrocellulose membranes (*Millipore* HAWP 025 00*)* and washed with a buffer containing 100 mM sodium acetate (*Sigma-Aldrich* S2889), 50mM magnesium chloride, and 50mM sodium sulfate (*Sigma-Aldrich* 239313) to eliminate the unincorporated ^{35}S-sulfate. The membranes were dissolved in scintillation fluid (*National Diagnostics* LS-201) and the counts per minute (CPM) are detected with the scintillation counter (*Packard* Tri-Carb 2100TR). CPM was converted to number of pmoles of sulfate, using the specific activity of ^{35}S-sulfate in the conditioned media, and then normalized to DNA amount via Picogreen assay (*Life Technologies* P7589).

RNA isolation was done using Qiagen RNeasy Plus Micro Kit (*Qiagen 74034*). Quantitative RT-PCR was performed using a one-step SYBR Green fluorescent reporter system

(*Bio-Rad* 1725151) with Bio-Rad iQ5 Multi-color Real-time PCR Detection System with 7 cycles: Cycle 1 (30 minutes @ 48º C), Cycle 2 (10 minutes @ 95ºC), Cycle 3 (15 seconds @ 95ºC then 1 minute @ 62ºC, repeated 30X), Cycle 4 (1 minute @ 95ºC), Cycle 5 (1 minute @ 55ºC), Cycle 6 (10 seconds @ 55ºC, repeated 80X), Cycle 7 (hold indefinitely @ 22ºC). Previously validated primers [80, 81] were used for key matrix components: Aggrecan, Collagen 1, Collagen 2, Versican, and Link Protein (Table 2). 30 ng of RNA per sample were analyzed. Melt curves were analyzed (Cycle 6) after amplification was complete and compared to RNA-negative water controls. For all experiments performed, there were either no products from the water control as signified by no peak or a non-specific primer dimer product that appeared as a distinct peak at a lower temperature shifted down from the specific cDNA products. The $2^{\Delta\Delta Ct}$ approximation method [82] was used for relative mRNA quantification for the specific products probed for in Table 1. The amplification efficiencies of the reference housekeeping gene and the target gene of interest must be approximately equal for this method to be valid.

Initially, GAPDH was used as a reference housekeeping gene for normalization of all other genes of interest in the $2^{\Delta\Delta Ct}$ approximation method. Untreated, negative control samples were used as the calibrator sample for normalization for all other samples of interest in the $2^{\Delta\Delta Ct}$ approximation method.

Table 2. Primers used for qRT-PCR for matrix anabolism and matrix catabolism

Gene [Homo sapiens (human)]	Forward (5' to 3')	Reverse (5' to 3')
ADAMTS-4	TCACTGACTTCCTGGACAATGG	ACTGGCGGTCAGCATCATAGT
ADAMTS-5	CTGACCTACCACGAAAGCAGATC	ATGCCGGACACACGGAGTA
Aggrecan	AAGAATCAAGTGGAGCCGTGTGTC	TGAGACCTTGTCCTGATAGGCACT
Collagen Type I, α1	GGAAACAGACAAGCAACCCAAACT	GGTCATGTTCGGTTGGTCAAAGATAA

Table 2. Continued

Collagen Type II, α1	ATGACAATCTGGCTCCCAAC	GAACCTGCTATTGCCCTCCTG
GAPDH	ACCCACTCCTCCACCTTTGAC	TCCACCACCCTGTTGCTGTAG
HAPLN1	GeneCopoeia Catalog#: HQP003013 Validated All-in-One™ qPCR Primer	
IL-6	AGCCACTCACCTCTTCAGAACG	TGCCTCTTTGCTTTCACAC
IL-8	GGCCGTGGCTCTCTTGGCAG	TGTGTTGGCGCAGTGTGGTCC
MMP-1	GAGCTCAACTTCCGGGTAGA	CCCAAAAGCGTGTGACAGTA
MMP-3	CAAGGAGGCAGGCAAGACAGC	GCCACGCACAGCAACAGTAGG
TIMP-1	TGGCTTCTGGCATCCTGTTGTTG	CGCTGGTATAAGGTGGTCTGGTTG
TIMP-3	AGGACGCCTTCTGCAACTC	GTACTGCACATGGGGCATCT
Versican	GCGGAGACCAGTGTGAACTTGATT	ACATAACTTGGAAGGCAGAGGCAC

3.4   MATRIX CATABOLISM: GENE EXPRESSION

RNA isolation was done using Qiagen RNeasy Plus Micro Kit. Quantitative RT-PCR was performed using a one-step SYBR Green kit (master mix and reverse transcriptase) with validated primers for MMPs, ILs, and ADAMTSs (Table 1). ELISA was performed with the conditioned media from 4 day incubation after the second hydrogen peroxide treatment of the NP cells using R&D Total Human IL-6, IL-8, MMP1, and MMP3 DuoSets (*R&D Systems* DY206, DY208, DY901, DY513).

3.5   MATRIX CATABOLISM: PROTEIN ARRAYS AND INFLAMMATION/MMP ARRAYS

Antibody arrays and western analyses were performed using concentrated conditioned media from human AF and NP cells with and without hydrogen peroxide oxidative stress treatment. Conditioned media was concentrated 3-5X using Millipore Amicon Ultra-15 Centrifugal Filter

Unit with Ultracel-3 (*EMD* Millipore UFC900308) membrane with 3 kDa molecular weight cut off – proteins smaller than 3 kDa excluded. For detection of aggrecan fragments, 1:1000 rabbit polyclonal anti-Aggrecan antibody (*Abcam* ab36861) was used as primary antibody followed with 1:10000 anti-rabbit goat secondary antibody with HRP (*Thermo Scientific* PI-31460) and chemiluminescent detection (*Thermo Scientific* 34096 and *Bio-Rad* ChemiDoc MP). Western was performed using Tris-HEPES 4-20% gradient gel (*Thermo Scientific* 25204), Tris-HEPES-SDS Running Buffer (*Thermo* 28398), Tris-Glycine Transfer Buffer with 10% Methanol (*Thermo Scientific* 28380, *Fisher Scientific* A452-4), and TBST (*Sigma-Aldrich* T9039). Antibody arrays were performed using human inflammation antibody array (*RayBioTech* AAH-INF-3-4) and human MMP antibody array (*RayBioTech* AAH-MMP-1-4) based on manufacturer's protocol instruction.

3.5.1 MMP Enzymatic Activity assay

Detection of a fluorogenic substrate cleavage product was used to assess MMP enzymatic activity [83]. Samples normalized to total protein were in serum free, phenol red free DMEM/F-12 (*Life Technologies* 11039-021) media (SF PF media). The stock substrate XI (*AnaSpec* 60578-01) was dissolved in 60 µL DMSO. The substrate working solution was prepared in a 1:50 dilution with 100 mM HEPES (*Sigma-Aldrich* H4034) in SF PF media. Seventy-five µL of each sample or media control was added to each well in duplicate in a black 96-well plate (*CoStar* 07- 200-590). Twenty- five µL of the substrate working solution was added to each well. Fluorescence was measured at 490nm excitation/520nm emission every 5 minutes for 1 hour. The resulting signal (after blank subtraction) is the Cleavage Product Fluorescence (CPF).

23

The slope for the linear regression line with y-intercept = 0 was calculated for CPF vs. time (min) each sample. The slopes were averaged for each duplicate. The slopes have the unit of mM fluorescent product/min, representing the MMP enzymatic rate.

3.6   TOTAL MATRIX CONTENT: DMMB GAG ASSAY

Colorimetric GAG (DMMB) assay was used to quantify total matrix content from ECM digestion buffer: 1mL 1M Sodium Acetate, 200 µL 0.5M EDTA (*Sigma-Aldrich* E6758), 100µL 1M L-cysteine (*Sigma-Aldrich* C7352), 100 µL 300 µg/ml Papain (*Sigma-Aldrich* P4762), 18.6 mL 55nM Citric Acid/150 mM Sodium Chloride pH 7.0 in addition to the 1,9-dimethylmethylene blue (DMMB) dye (for 1 liter: 21 mg DMMB (*Sigma-Aldrich* 341088), 5 mL 100% ethanol (*Sigma-Aldrich* E7023), 2 g sodium formate (*Sigma Aldrich* 71539), 800 mL water, ~200 mL formic acid (*Sigma-Aldrich* F0507) for pH adjust to 1.5, adjust to 1 L total volume with water (protect from light and lower temperatures). ECM digestion buffer was added to cell culture plate wells and incubated at 37°C (non-CO_2 incubator) for 6 hours before sample collection and DMMB assay. Standard curve were created using known concentrations of chondroitin sulfate in a serial dilution. Total GAG content was normalized to DNA measured by the Picogreen assay.

3.7   STATISTICAL ANALYSIS

Statistical analysis was performed using the software R. The statistical tests performed for the results include: Student's one-sample T-test (when assumptions are met), Student's paired T-test, and Wilcoxon Signed Rank test. All statistical tests were two-tailed tests. The assumptions of Student's T-test include equality of variance between arms/groups and Gaussian-ness/normality or residuals. These assumptions were checked using plots of residuals vs. fitted values and Quantile-Quantile (Q-Q) plots of standardized residuals for the data for each outcome measure. The regression diagnostics output four plots: Residuals vs. Fittted, Q-Q Plot of Standardized Residuals, Scale-Location Plot, and Leverage plots. The scale-location plot is in the upper left displays the residual errors plotted versus their fitted values. For the equality of variance assumption to be met, the residuals should be randomly distributed around the horizontal line representing a residual error of zero meaning there should not be skewedness or a trend in the distribution of points. Since any generated data is equal to signal measured plus noise (also known as residual = $y_i - \hat{y}$) and bias, the Q-Q plot of residuals should have most of the points falling on or near the line for the Gaussian-ness of residuals assumptions to be met. The scale-location plot is in the bottom showing the square root of the standardized residuals against fitted values with no obvious trend in the distribution of points. The constant leverage plot in the bottom right discloses more details about each datum and can help identify outliers. '*' indicates significance (p-value less than 0.05).

3.7.1 Statistical Analysis: PG Synthesis

For the PG Synthesis data, there appears to be a leverage point in the upper right of the Q-Q plot of residuals and residuals vs. fitted values plot (Figure 6). The range of the variances is a little troubling due to this leverage point. The rest of the data in the Q-Q plot of residuals appears to be Gaussian such that the normality of residuals assumption is roughly met. The other data in the residuals vs. fitted plot appears to be somewhat acceptable for the equality of variance assumptions. However, normalizing each senescent sample to the control sample from the same patient reduced this variance by quite a bit (Figure 6B). Therefore, it is a rough assumption that normalizing each senescent sample contributed to reducing the influence of the potential leverage points.

To remain conservative, a non-parametric Wilcoxon Signed Rank test was performed. The null hypothesis is there is no difference in the mean of PG synthesis normalized to DNA between the senescent disc cells and non-senescent, control disc cells (means are equal). The alternative hypothesis is there is a difference between the mean of PG synthesis normalized to DNA between the two groups (means are not equal such that the difference is non-zero).

For the ratio PG synthesis data, the null hypothesis is the mean ratio of senescent to control PG synthesis normalized to DNA is equal to one while the alternative is that the mean ratio not equal to one.
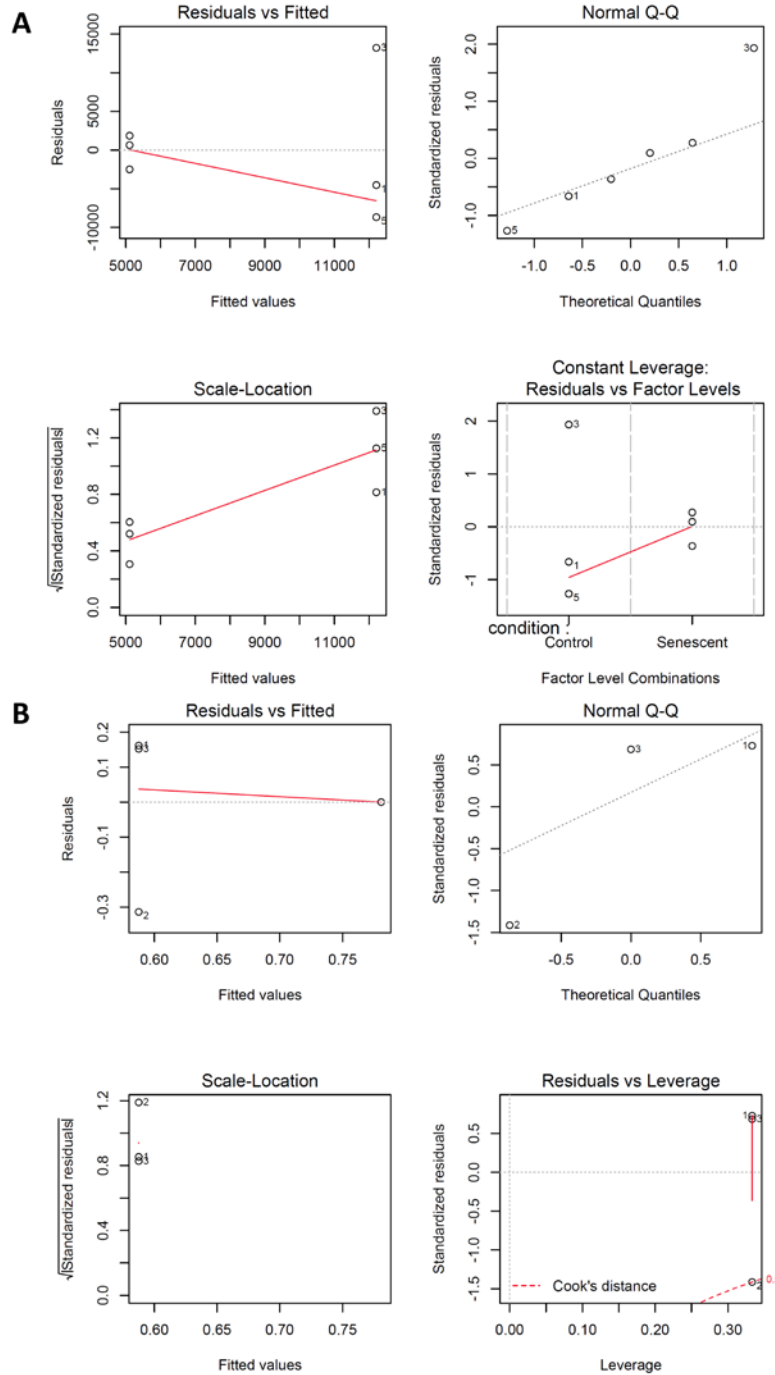
(A) Regression diagnostics for the total GAG content for senescent and control samples. (B) Regression diagnostics for the ratio of senescent to control samples (total GAG content). A datum was entered for one hNP sample for data we had collected for the linear model of GAG ratio (senescent to control) vs. cell type as represented by the rightmost point in the Residuals vs. Fitted plot.

Figure 6. Regression diagnostics for GAG (DMMB) assay with senescent and non-senescent control hAF samples (n=3).

3.7.2 Statistical Analysis: PCR for Anabolic Genes

The equality of variance assumption was met for all anabolic genes for hAF (Figure 7) and hNP (Figure 8) in the exponential scale (ΔC_t). The normality of residuals assumption was approximately met for hAF (Figure 7) and hNP (Figure 8) in the exponential scale (ΔC_t). However, transforming to the linear scale makes the distribution of the residuals more non-Gaussian and variances more unequal (Figure 9 and 10). Essentially, normalizing to the calibrator sample is a similar transformation to the ratio mentioned for the statistical analysis of PG synthesis where two sets of values for two conditions becomes one set of values for one normalized condition (senescent to control). Therefore, the calibrator (control) samples in relative quantitative RT-PCR are denoted a value of 1 and as such causes the inequality of variances and non-Gaussian-ness of residuals in regression diagnostics. With this caveat, the assumptions for the t-test are met in the exponential scale, but not in the linear scale by the nature of the $2^{\Delta\Delta Ct}$ approximation method [82]. Since this method is widely accepted for analyzing relative gene expression, such scrutiny of the t-test assumptions may not be required in this particular case. Overall, due to the previously established $2^{\Delta\Delta Ct}$ approximation method, Student's paired t-test was used for the relative expression ($2^{\Delta\Delta Ct}$) values for each condition. The null hypothesis is the mean difference between the senescent and control groups for relative gene expression is zero. Of course, this is somewhat arbitrary due to calibrator/control samples being assigned a value of 1. Therefore, the null hypothesis may instead be taken as the mean relative gene expression for the senescent is equal to one (and alternative is that the mean is not equal to one).

Alternatively, the mean ΔΔCt can be used in the null hypothesis where the mean ΔΔCt between treated and calibrator sample is zero for a one-sampled T-test. Also, the ΔCt values can be compared between treated and calibrator samples such that the null hypothesis for a paired T-test is the mean difference between ΔCt values is equal to zero.
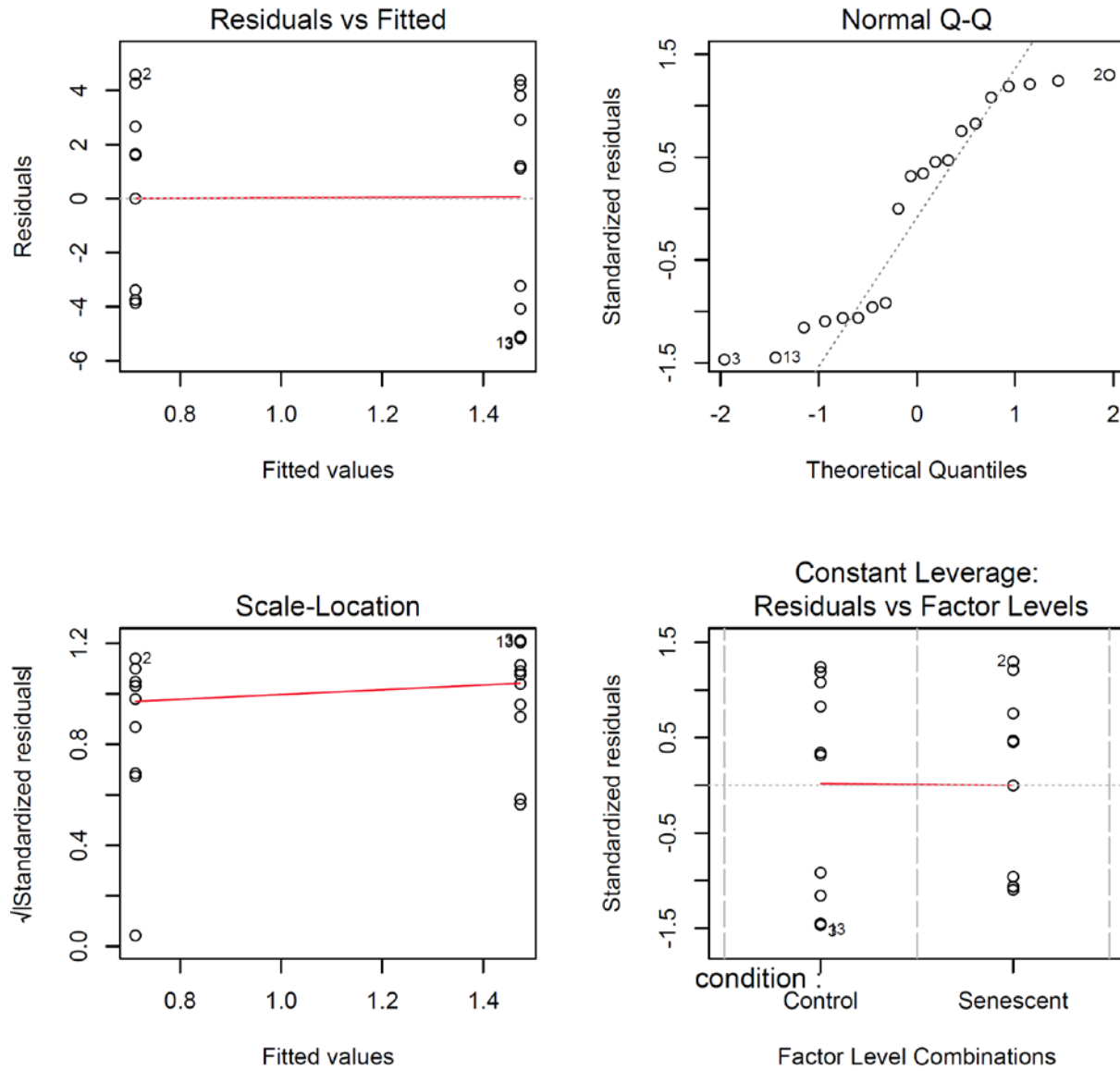
Figure 7. Regression Diagnostics for ΔCt values for hAF senescent and control samples for anabolic genes (exponential scale).
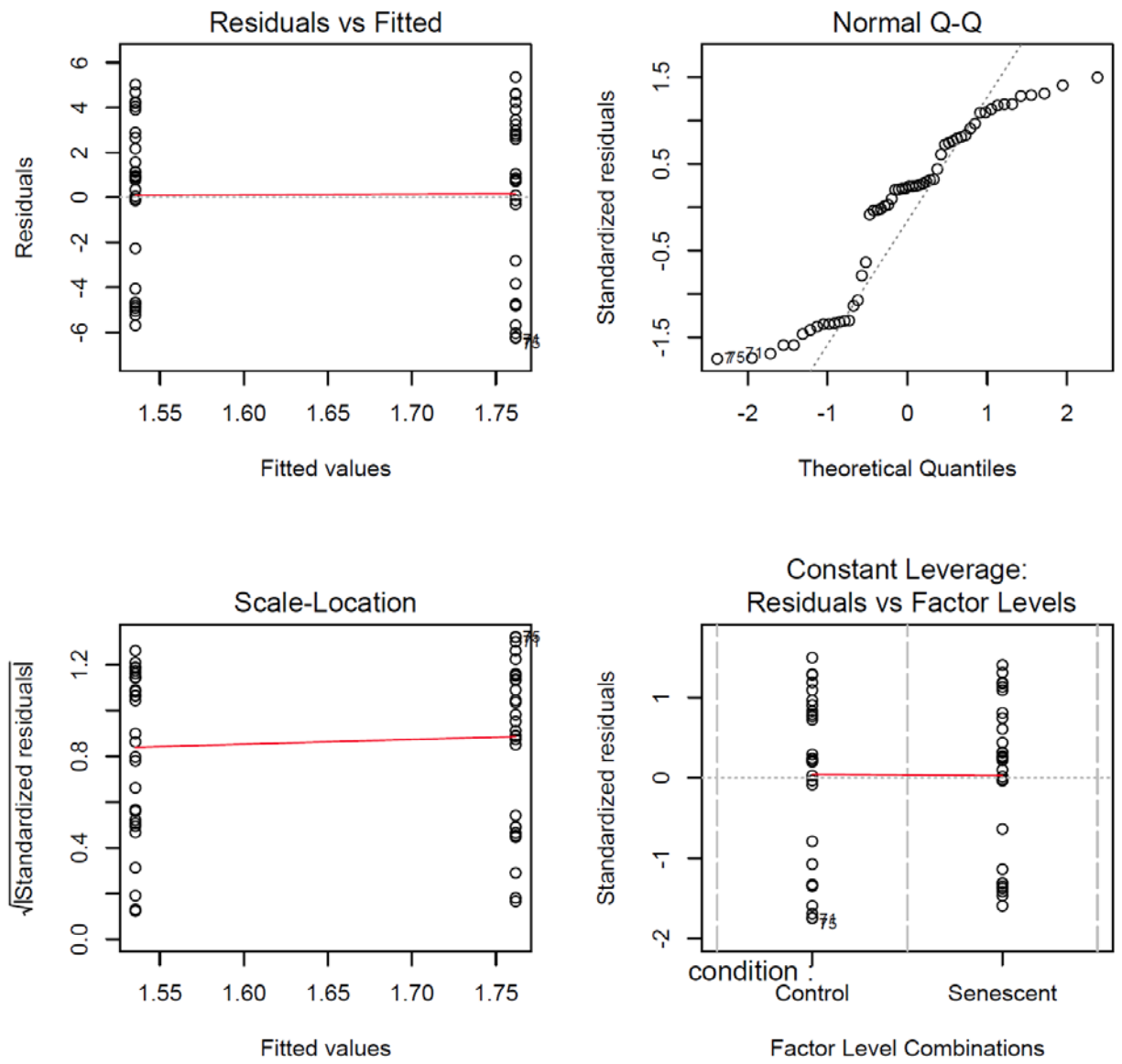
Figure 8. Regression Diagnostics for ΔCt values for hNP senescent and control samples for anabolic genes (exponential scale).
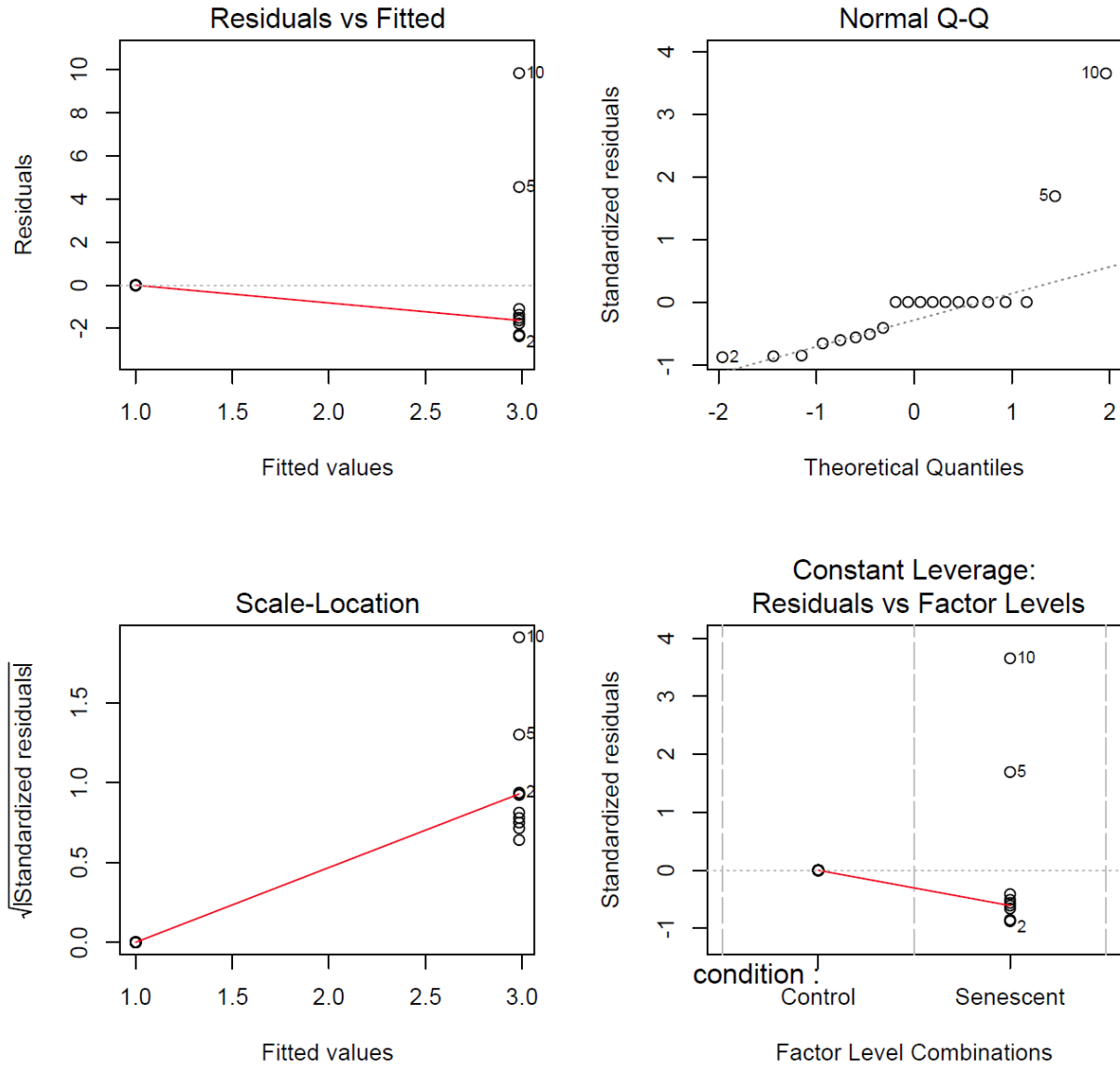
Figure 9. Regression diagnostics for relative gene expression ($2^{\Delta\Delta Ct}$) for hAF senescent and control samples for anabolic genes (linear scale)
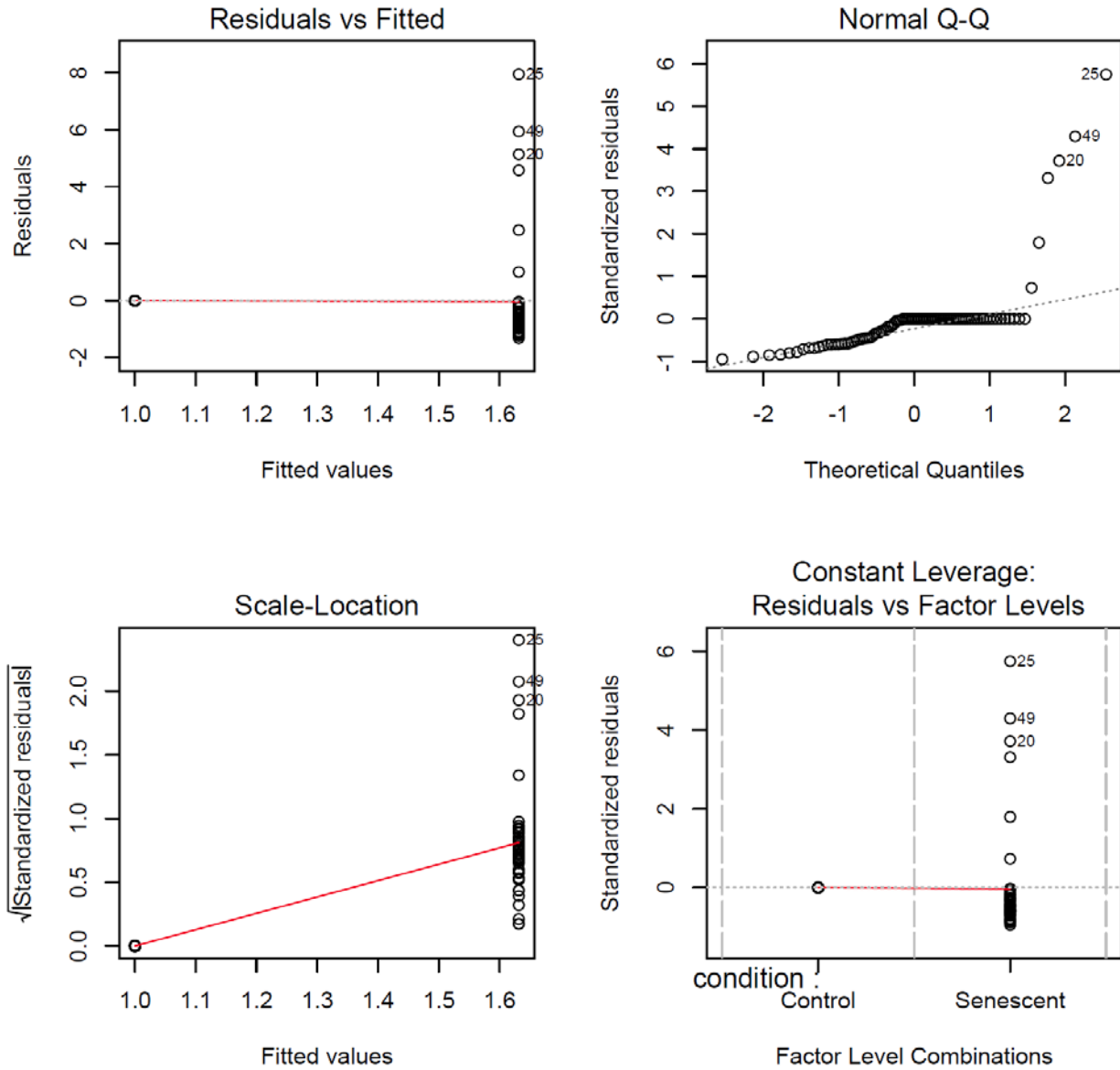
Figure 10. Regression diagnostics for relative gene expression ($2^{\Delta\Delta Ct}$) for hNP senescent and control samples for anabolic genes (linear scale)

33

3.7.3   Statistical Analysis: PCR for Catabolic Genes

The regression diagnostics for PCR with catabolic genes shows the same result as PCR with anabolic genes. The assumptions are met quite well in the exponential scale (Figure 11), but not as much in the linear scale (Figure 12). Overall, due to the previously established $2^{\Delta\Delta Ct}$ approximation method, Student's paired t-test was used for the relative expression ($2^{\Delta\Delta Ct}$) values for each condition.
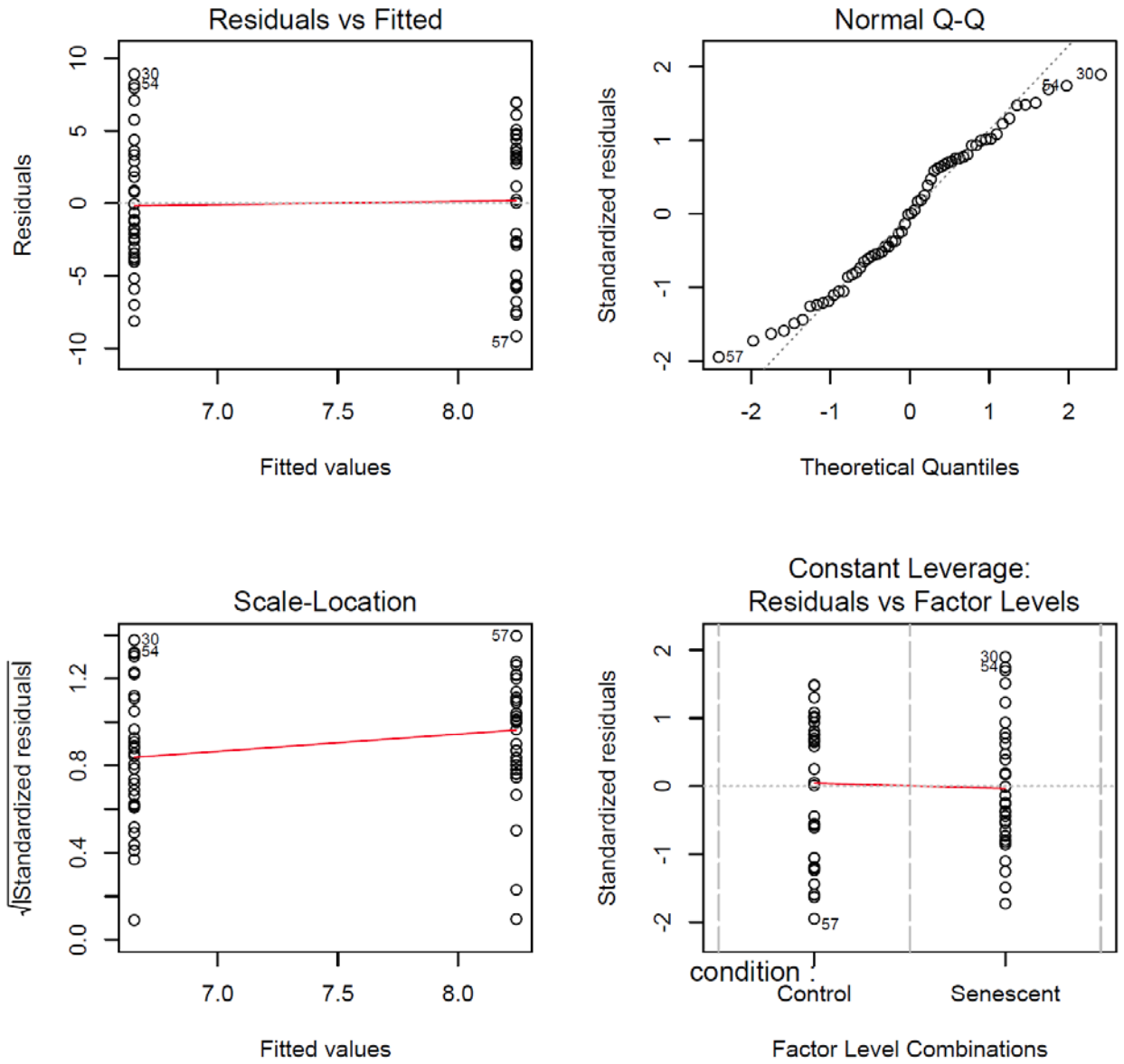
Figure 11. Regression diagnostics for ΔCt values for hNP senescent and control samples for catabolic genes (exponential scale).
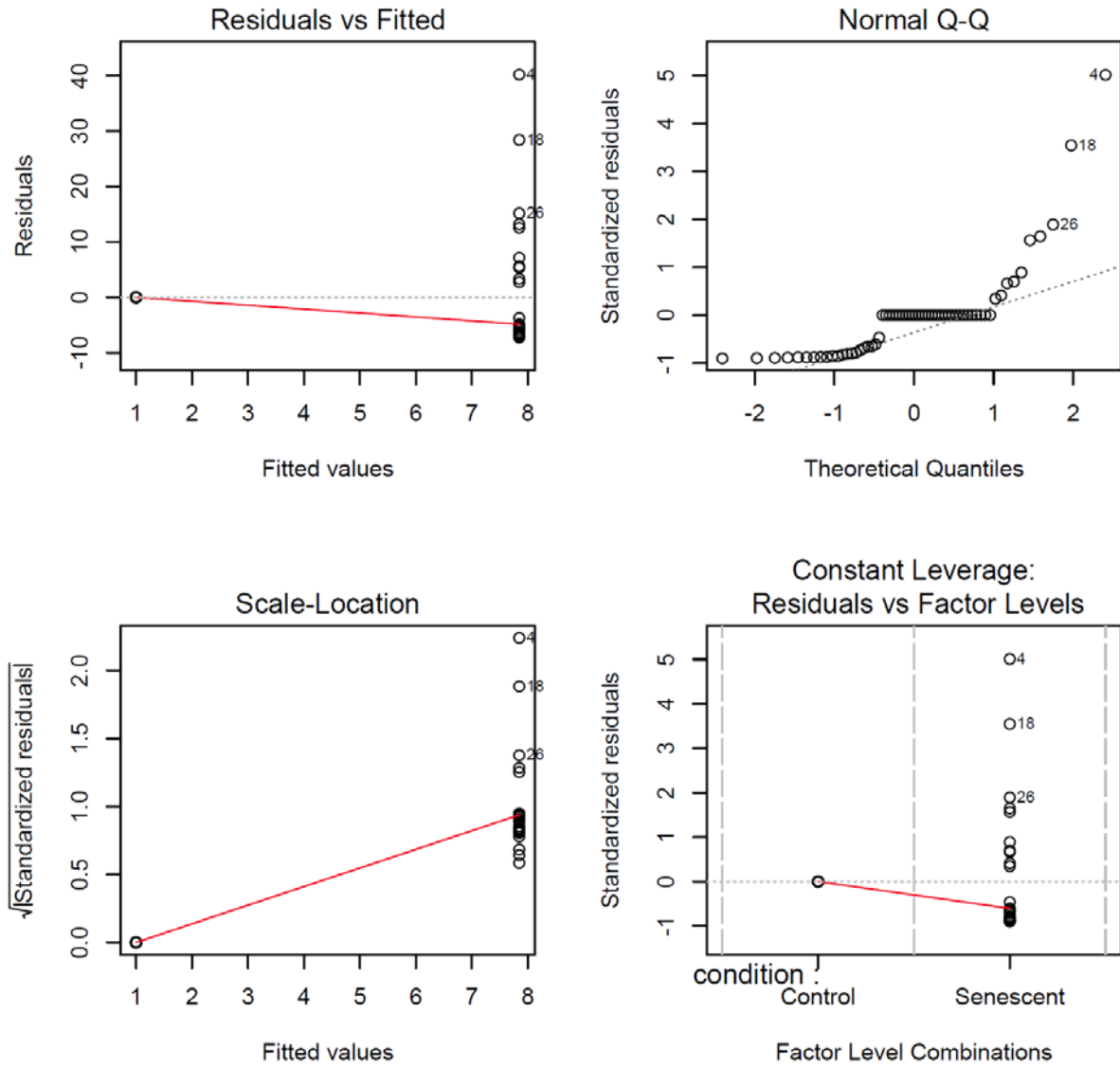
Figure 12. Regression diagnostics for relative gene expression ($2^{\Delta\Delta Ct}$) for hNP senescent and control samples for catabolic genes (linear scale).

3.7.4 Statistical Analysis: ELISA (Catabolic)

The regression diagnostics for MMP-1 (Figure 13) and MMP-3 (Figure 14) show the equality of variance assumption (residual vs. fitted plot) is met, but the Gaussian-ness of residuals assumption is not met (Q-Q plot of residuals). Therefore, for MMP-1 and MMP-3, the non-parametric alternative to Student's paired T-test. Wilcoxon Signed Rank test was used over the paired T-test.

The regression diagnostics for IL-6 (Figure 15) and IL-8 (Figure 16) show the equality of variance assumption (residual vs. fitted plot) is met as well as the Gaussian-ness of residuals assumption (Q-Q plot of residuals). Therefore, for MMP-1 and MMP-3, the non-parametric alternative to Student's paired T-test, Wilcoxon Signed Rank test was used over the paired T-test.

The null hypothesis was there is no difference in the mean protein level (MMP-1, MMP-3, IL-6, IL-8) between senescent and control samples. The alternative was there is a difference between mean protein levels for the two groups.
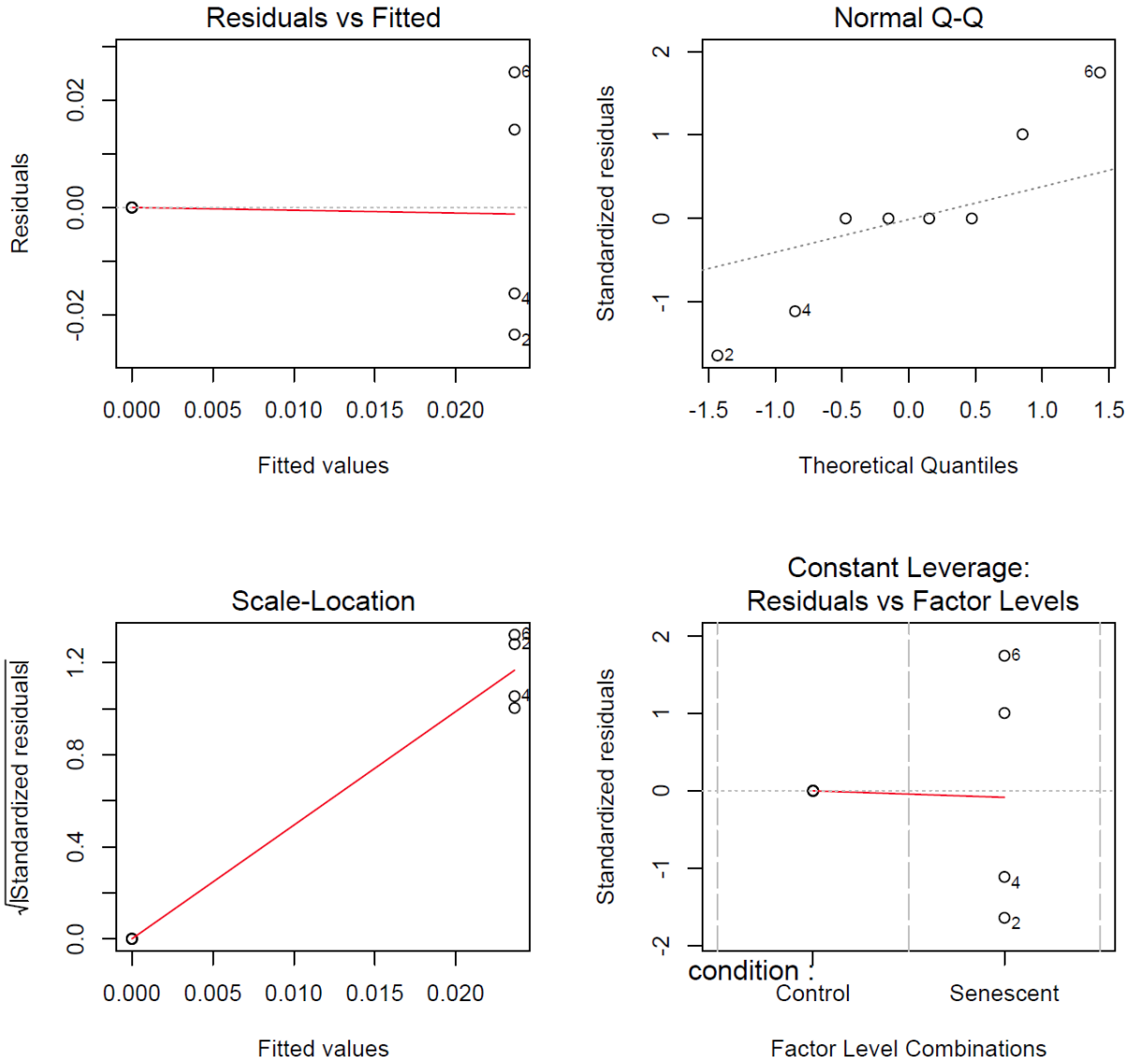
Figure 13. Regression diagnostics for MMP-1 ELISA for hNP senescent and control conditioned media
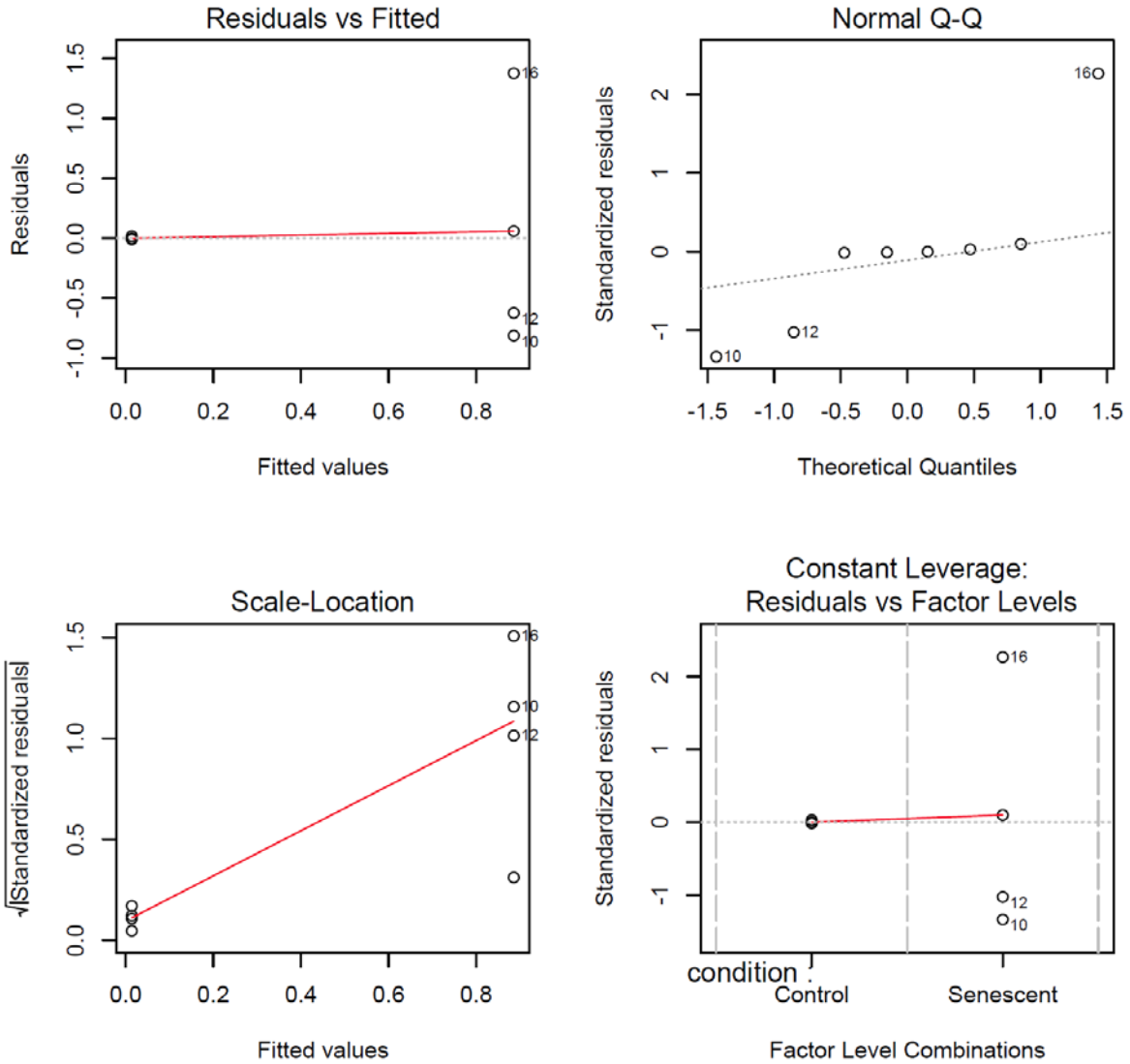
Figure 14. Regression diagnostics for MMP-3 ELISA for hNP senescent and control conditioned media
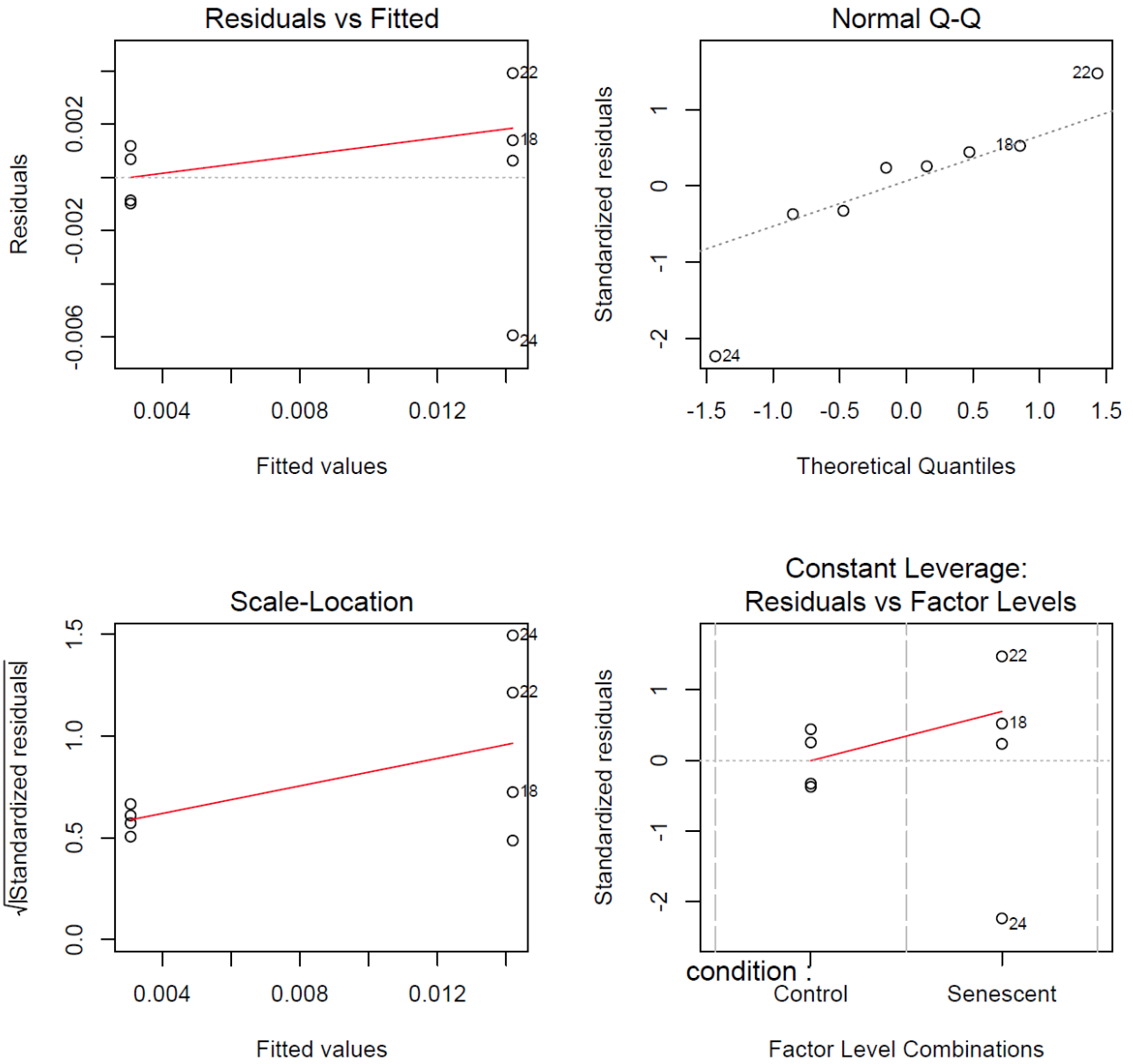
Figure 15. Regression diagnostics for IL-6 ELISA for hNP senescent and control conditioned media
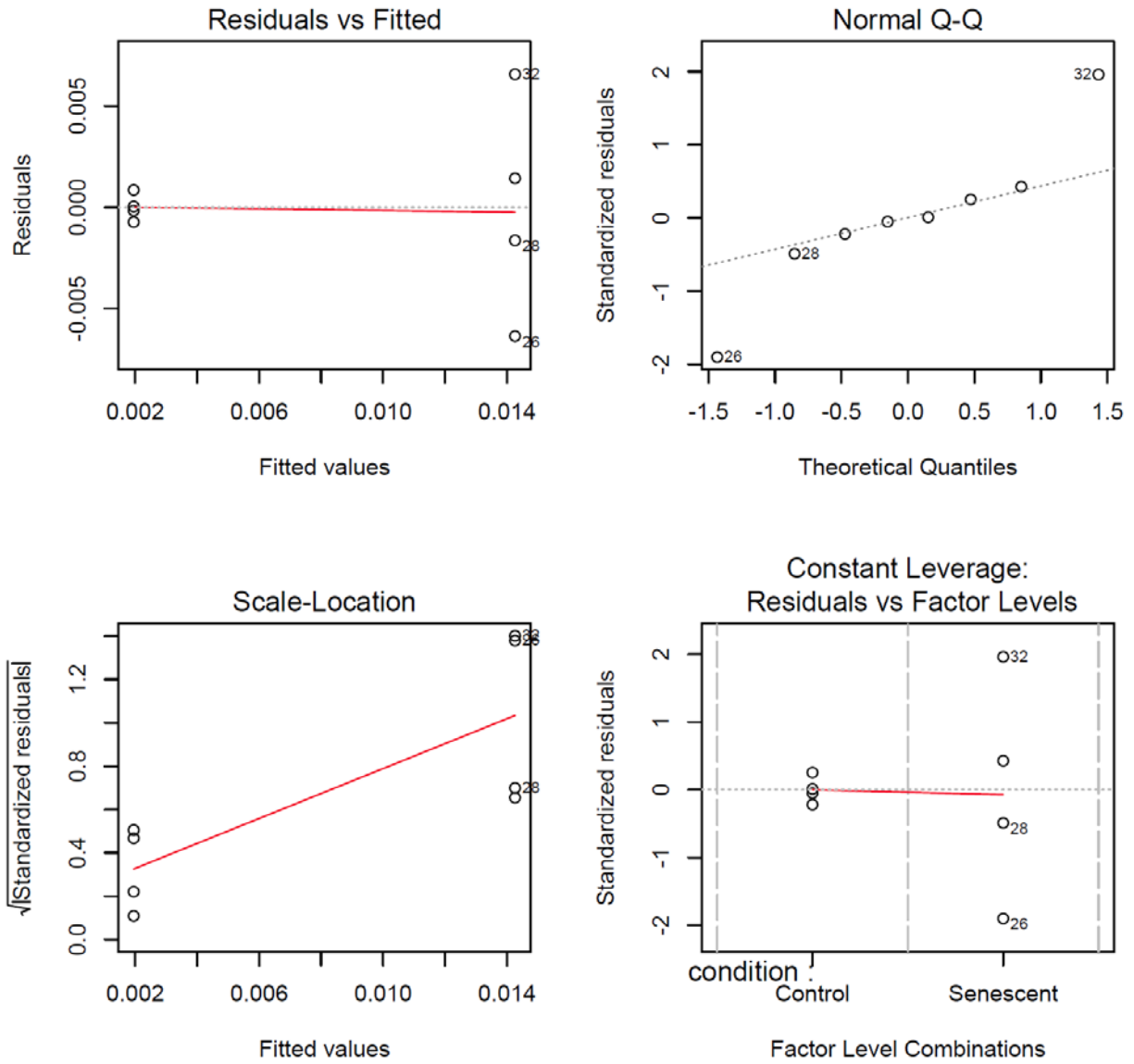
Figure 16. Regression diagnostics for IL-8 ELISA for hNP senescent and control conditioned media

3.7.5 Statistical Analysis: Western Detection of Aggrecan

The regression diagnostics for the densitometry of the ADAMTS-generated (Figure 17) and MMP-generated (Figure 18) aggrecan fragments detected by Western were quite exceptional in terms of meeting the T-test assumptions of equality of variance (residuals vs. fitted plot) and normality of residuals (normal Q-Q plot of residuals). Therefore, Student's one-sample T-test was performed. The null hypothesis was there is a difference of zero between the mean ADAMTS-generated and MMP-generated aggrecan fragments from the senescent and control samples. The alternative hypothesis was there is a difference. For the ratio, the null hypothesis is that the mean ratio of senescent to control is equal to one while the alternative hypothesis is that the ratio of senescent to control is not equal to one.
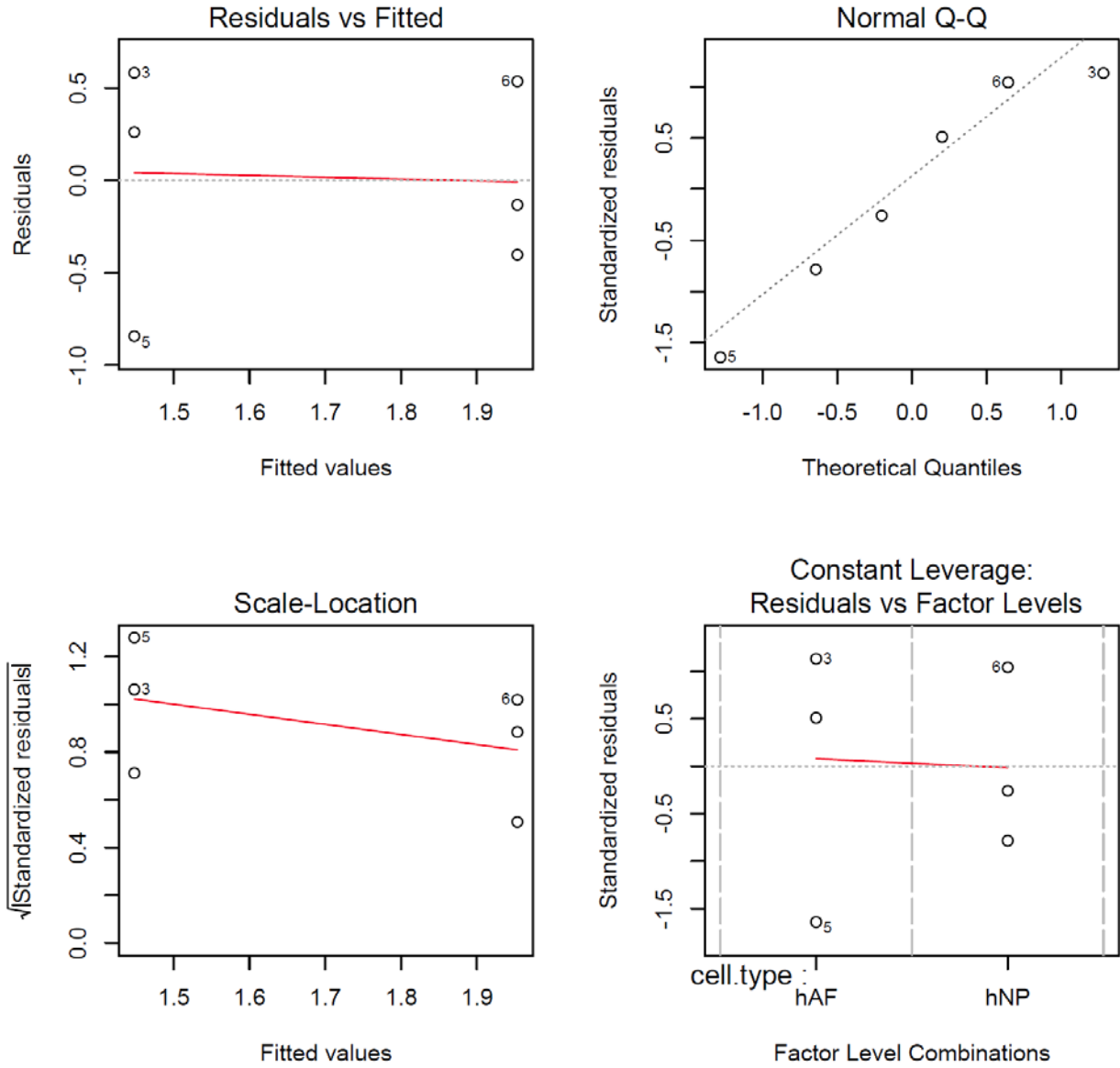
Figure 17. Regression diagnostics for ADAMTS-generated fragment from Western detection of Aggrecan for hNP senescent and control conditioned media (ratio of senescent to control).
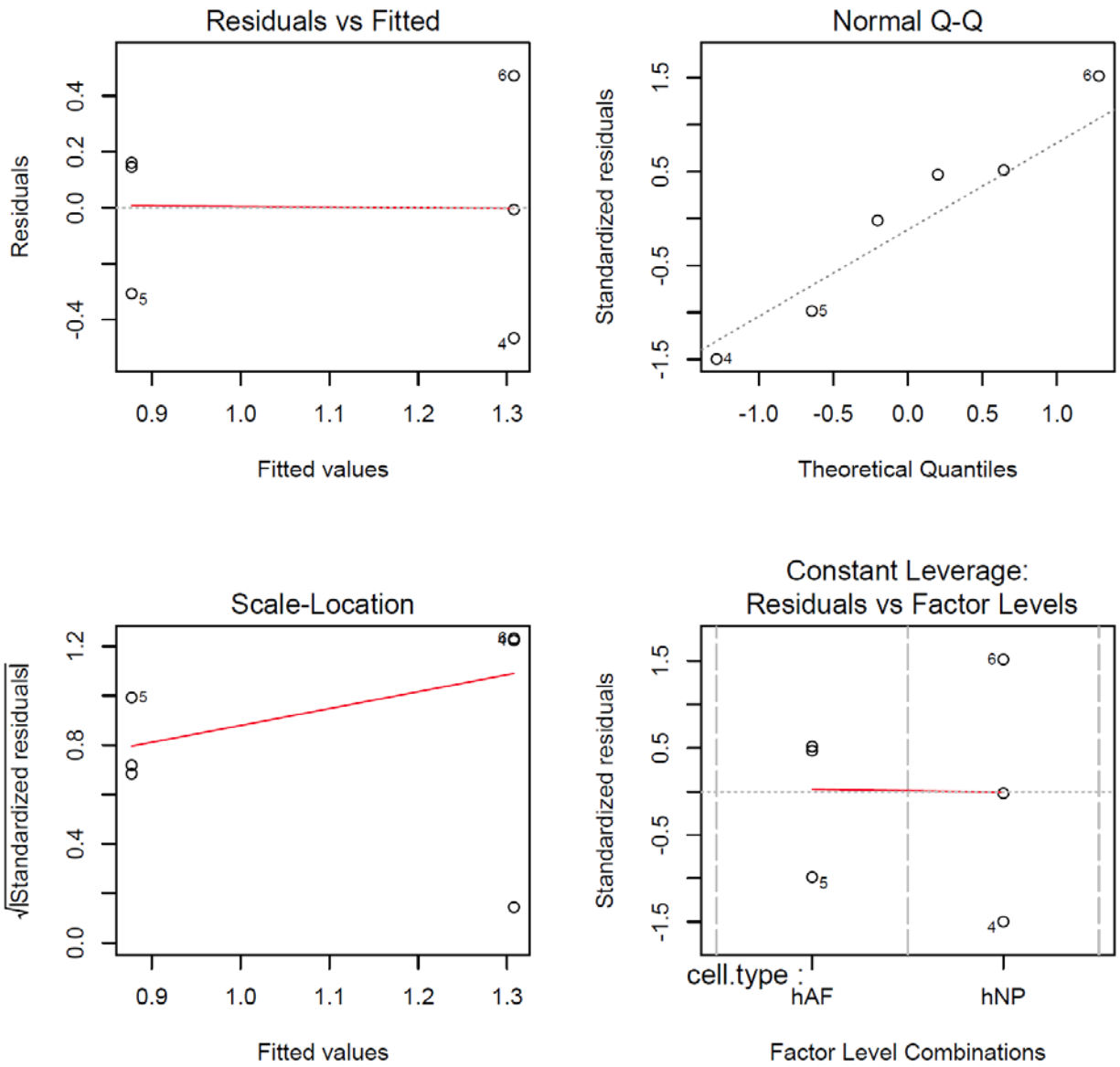
Figure 18. Regression diagnostics for MMP-generated fragment from Western detection of Aggrecan for hNP senescent and control conditioned media (ratio of senescent to control).

3.7.6   Statistical Analysis: Inflammation Antibody Array

The regression diagnostics show some inequality of variance (residuals vs. fitted), but approximately Gaussian residuals other than the tails (Q-Q plot) (Figure 19). However, besides the few potential leverage points, the assumptions are very roughly met such that Student's one-sample T-test is somewhat appropriate to perform. For the ratio, the null hypothesis is that the mean ratio of senescent to control is equal to one while the alternative hypothesis is that the ratio of senescent to control is not equal to one.
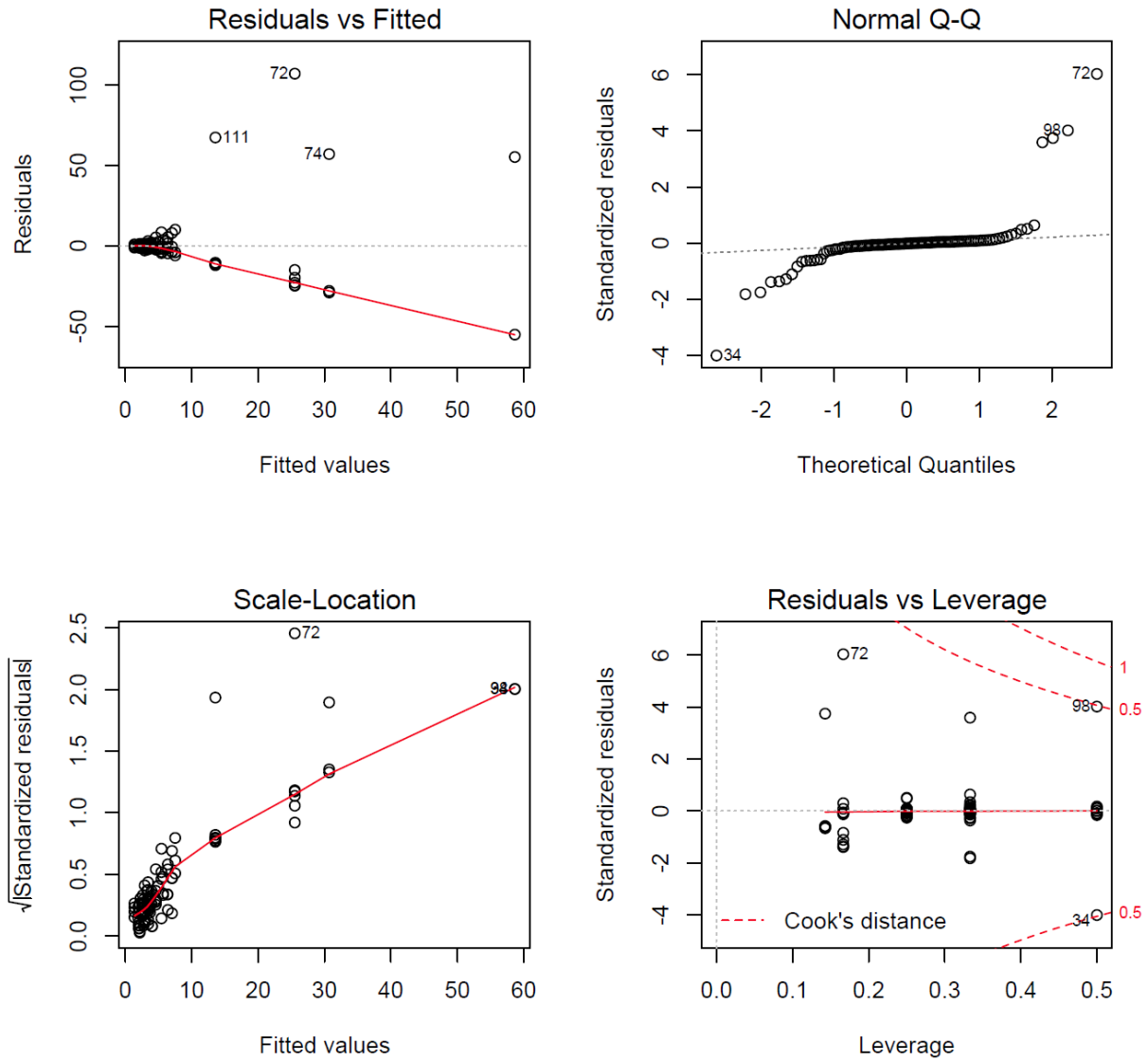
Figure 19. Regression diagnostics for Inflammation Antibody Array for hNP senescent and control conditioned media (ratio of senescent to control) for all targets.

3.7.7   Statistical Analysis: MMP Antibody Array

The regression diagnostics show some equality of variance (residuals vs. fitted) and approximately Gaussian residuals other than the tails (Q-Q plot) (Figure 20). The assumptions appear to be met such that Student's one-sample T-test is appropriate to perform. For the ratio, the null hypothesis is that the ratio of senescent to control is equal to one while the alternative hypothesis is that the ratio of senescent to control is not equal to one.
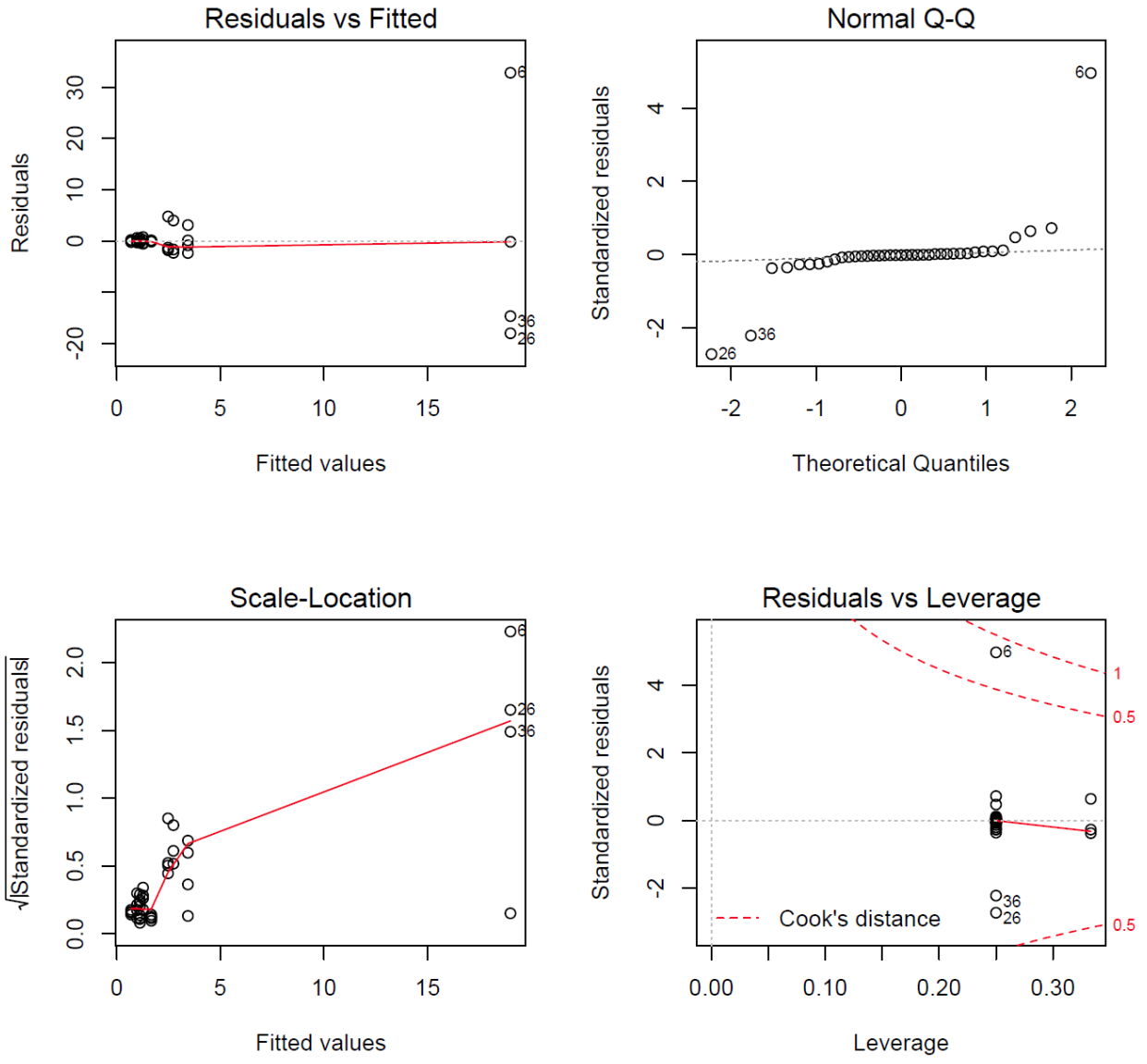
Figure 20. Regression diagnostics for MMP Antibody Array for hNP senescent and control conditioned media (ratio of senescent to control) for all targets.

3.7.8 Statistical Analysis: MMP Enzymatic Activity Assay

The regression diagnostics for MMP enzymatic activity assay revealed an approximately normality of residuals and equality of variance for hAF and hNP samples (Figures 21 and 22) such that Student's paired T-test is appropriate to perform. The null hypothesis is that the mean MMP enzymatic activity of senescent disc cells equals the man MMP enzymatic activity of untreated, non-senescent control disc cells. The alternative hypothesis is that the mean MMP activity of senescent disc cells is not equal to the mean MMP activity of non-senescent control disc cells.
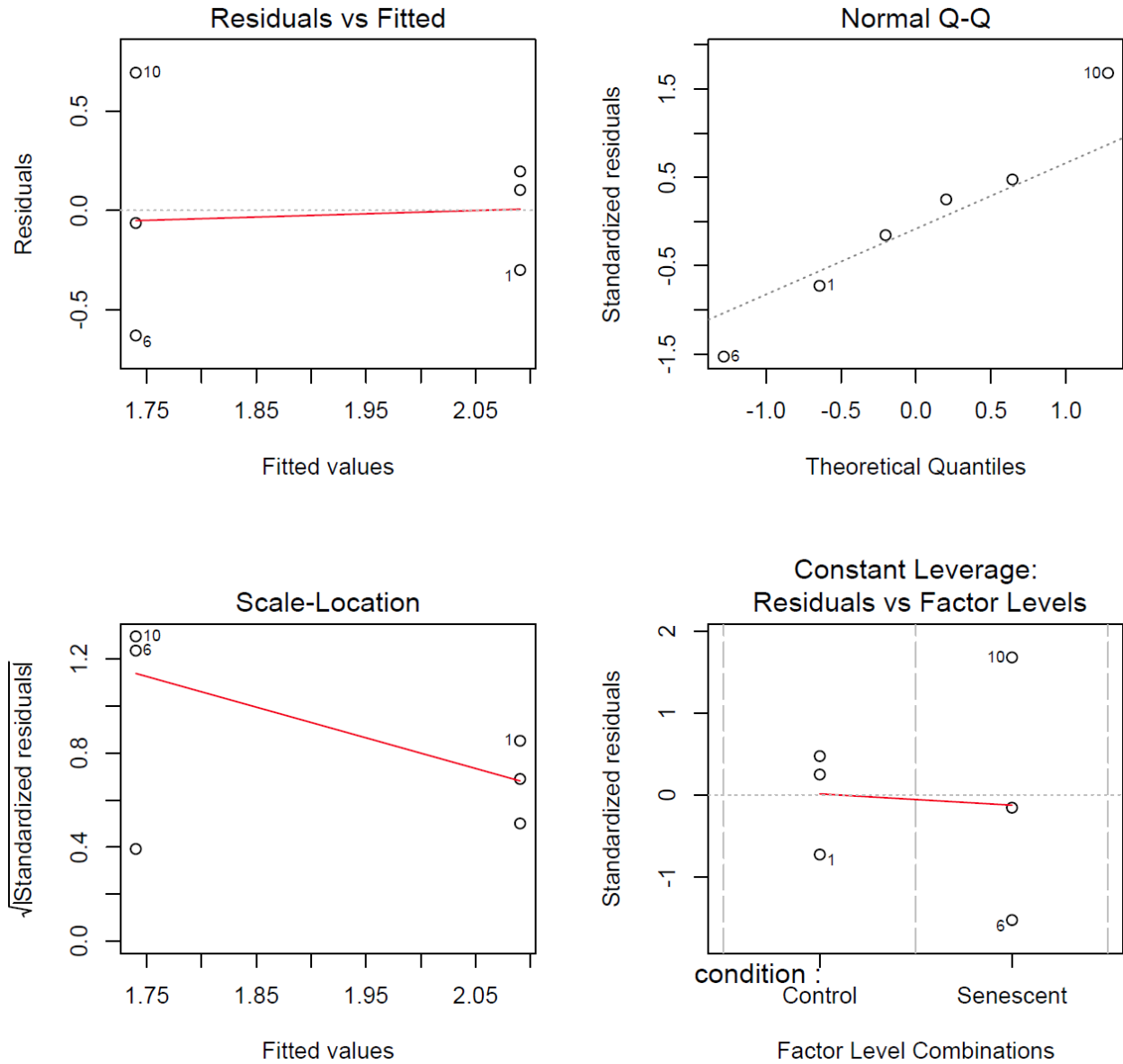
Figure 21. Regression diagnostics for MMP Enzymatic Activity for hAF senescent and control conditioned media (ratio of senescent to control) for all targets.
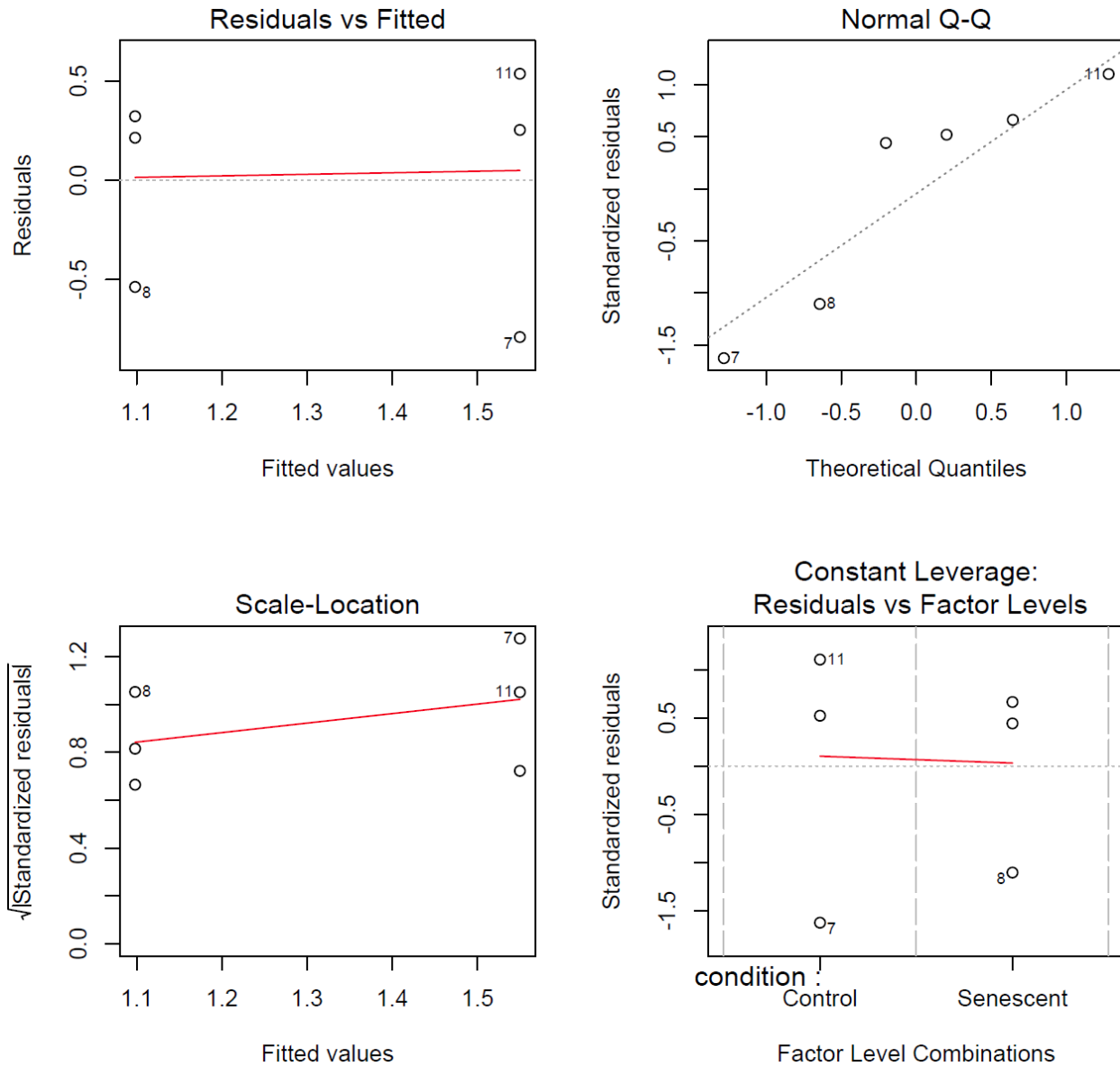
Figure 22. Regression diagnostics for MMP Enzymatic Activity for hNP senescent and control conditioned media (ratio of senescent to control) for all targets.

3.7.9   Statistical Analysis: GAG (DMMB) Assay

The regression diagnostics were acceptable with rough equality of variance and normality of residuals with a potential leverage point (Figure 23). Due to the paired nature of the hAF and hNP isolated from the same patients, the potential leverage point was not removed from the data set. Therefore, with assumptions being roughly met, Student's one-sample T-test was performed. The null hypothesis was there is a difference of zero between the mean total GAG content normalized to DNA from the senescent and control samples. The alternative hypothesis was there is a difference. For the ratio, the null hypothesis is that the ratio of senescent to control is equal to one while the alternative hypothesis is that the ratio of senescent to control is not equal to one.
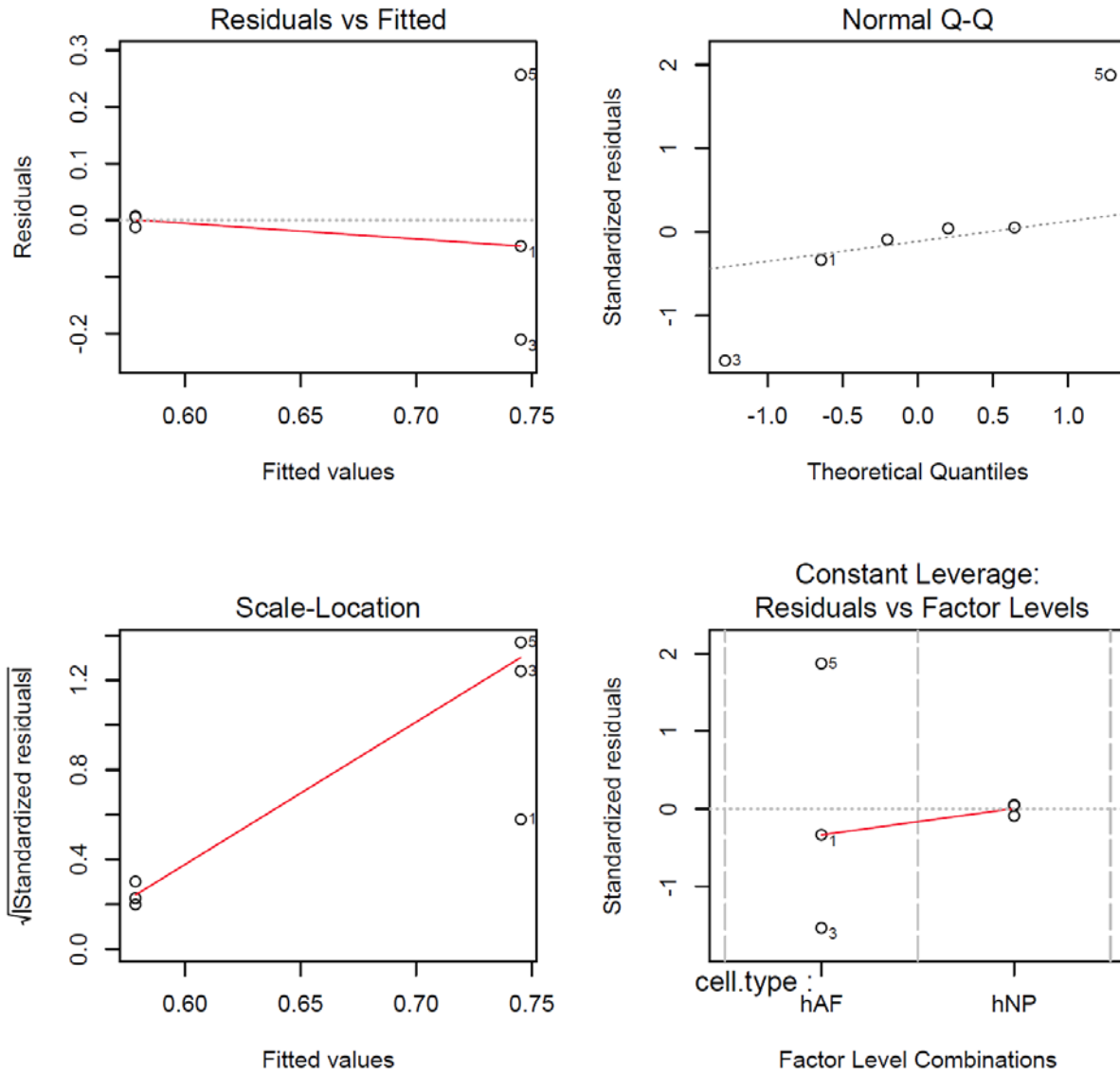
Figure 23. Regression diagnostics for GAG assay Activity for hAF and hNP senescent and control conditioned media (ratio of senescent to control) for all targets.

4.0   RESULTS

4.1   CONFIRMATION OF SENESCENCE INDUCTION

4.1.1   SA-β-Galactosidase Staining

To induce senescence, human disc cells were exposed to hydrogen peroxide for 2 hours then changed to regular media F-12 10% FBS 1% PS, split onto new plates, incubated overnight, treated with hydrogen peroxide again for two hours, changed to fresh media, and incubated for 4 days before sample collection and analysis to allow enough time for the development of SASP. To confirm senescence, SA β-gal staining was performed, and the results showed that a majority of the hydrogen peroxide treated cells were positive for SA β-gal activity along with enlarged flattened morphology (Figure 24). The hydrogen peroxide-treated cells also exhibited growth arrest as assessed qualitatively via microscopy (Figure 24). These features are consistent with those seen in senescent cells, which reportedly have the characteristics of enlarged morphology, increased senescence-associated β-galactosidase activity, nuclear DNA damage foci, p16 expression, and changes in chromatin organization and gene expression [67].
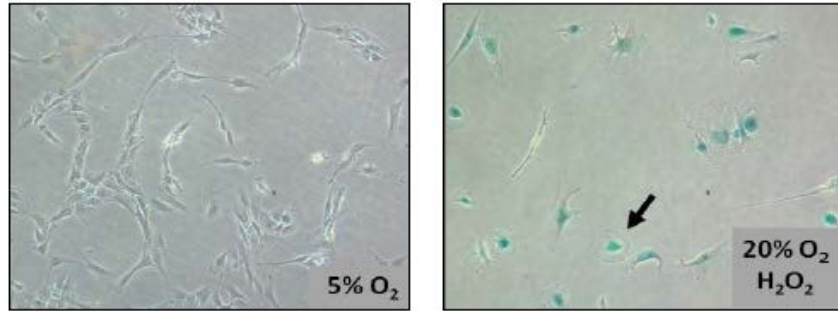
Compared to untreated control (left), nearly all the cells in human disc monolayer cultures consecutively exposed to 0.5mM H_2O_2 entered senescence (right), as evidenced by SA β-gal activity staining (blue) and cell morphological changes (flat pancake appearance). Representative images taken from one donor (n=4).
Figure 24. Oxidative stress-induced disc cellular senescence.

4.2   MATRIX ANABOLISM

4.2.1   PG Synthesis

To assess matrix anabolism, ^{35}S-sulfate incorporation assay for hAF and hNP senescent and untreated control cells was performed. Senescent disc cells showed a non-significant decreasing trend of PG synthesis by about 2.5x compared to untreated, non-senescent control cells (Figure 25A) with a mean ratio of approximately 0.6 for senescent to control (Figure 25B). This non-significant result trends toward the expected outcome of senescent disc cells in producing less new PG matrix compared to non-senescent control cells proposed in specific aim 1.

A PG Synthesis normalized to DNA

B Ratio SENESCENT:CONTROL (PG Synthesis normalized to DNA)
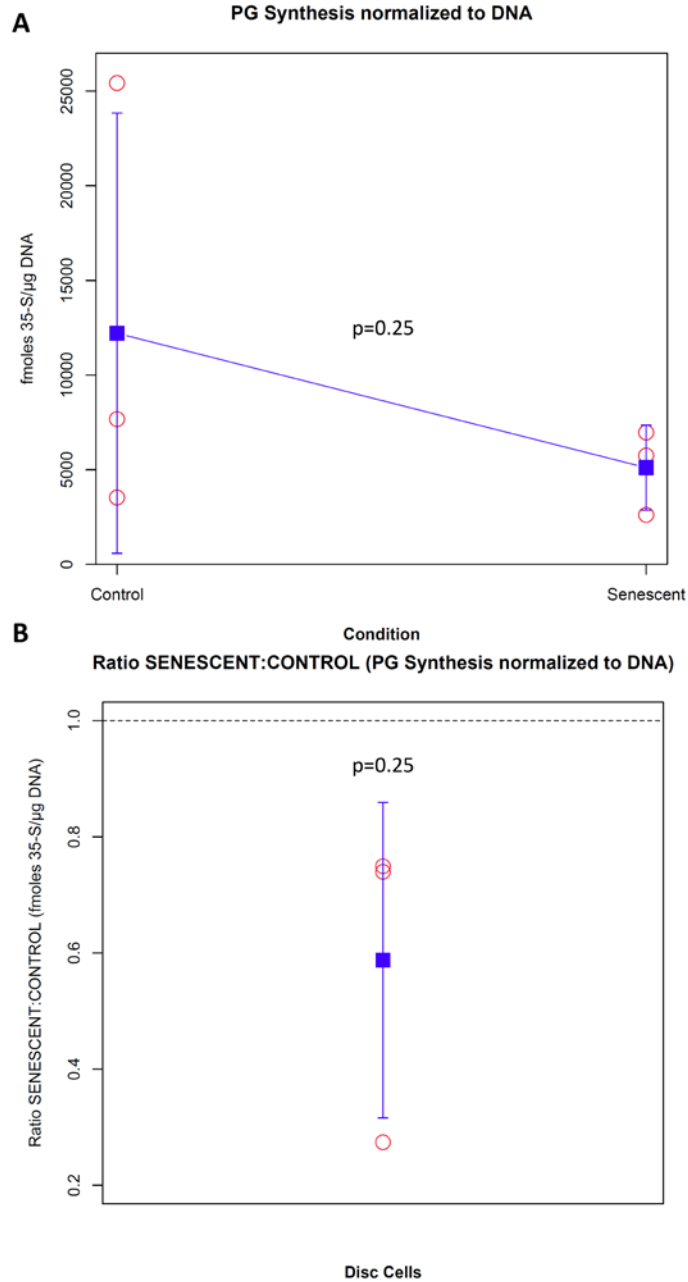
(A) H$_2$O$_2$–induced senescent disc cells incorporated 5100 ± 750 fmoles ^{35}S-sulfate/mg DNA, about two-fold lower than that seen in untreated non-senescent disc cells (12200 ± 3800). (B) Ratio of senescent to control. Dotted line represents ratio of 1 denoting no change. Blue square represents mean. Error bars represent SEM (n=3).
Figure 25. Oxidative stress-induced senescent disc cells displayed reduced PG synthesis.

4.2.2 PCR Anabolic Genes

To assess matrix anabolism, qRT-PCR was performed for key matrix component genes Aggrecan, Collagen Type I, Collagen Type II, Hyaluronan and Proteoglycan Link Protein 1 (HAPLN1), Versican. In hAF, collagen type I (p = 0.02936) expression decreases by 32.5% (Figure 26A) in senescent cells compared to control cells. In hNP, collagen type II (p = 0.03148) expression increases by 10-fold (Figure 26B) in senescent cells compared to control cells. Senescent hAF cells also trended towards an increase of collagen type II expression (non-significant, p = 0.1783), which may be non-significant due to the large variance in the donor samples for collagen type II expression compared to the small variance in the donor samples for collagen type I expression. The remaining matrix genes aggrecan, HAPLN-1, and versican remained relatively unchanged in senescent hAF and hNP cells compared to their non-senescent counterparts, with the exception of aggrecan trending towards increased expression in hAF (Figure 26). The expected outcome was decreased anabolic matrix gene expression, which is not the case observed for aggrecan, link protein, and versican. In hAF, there appears to be a divergence in collagen type I (decrease) and collagen type II (increase) expression while the only change for hNP is increase in collagen type II expression.
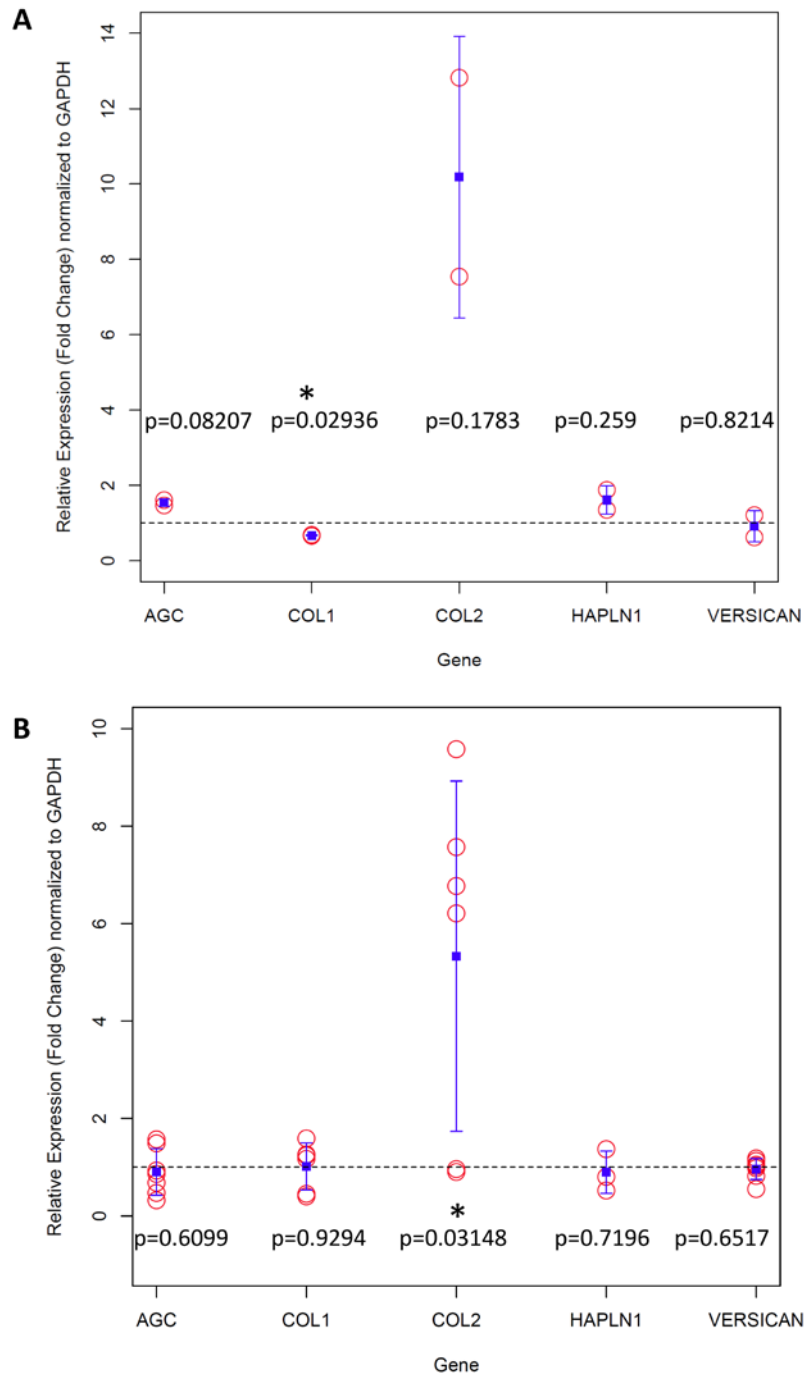
(A) hAF. (B) hNP. Aggrecan, Link Protein, and Versican matrix genes remain relatively unchanged for both hAF and hNP. Dotted line represents ratio of 1 denoting no change. Blue square represents mean. Error bars represent SEM (hAF n=2, hNP n=3 to n=6).
Figure 26. Oxidative stress-induced senescent disc cells displayed decreased Collagen Type I in hAF and increased Collagen Type II in hNP.

4.3   MATRIX CATABOLISM

4.3.1   PCR Catabolic Genes

To assess matrix catabolism, qRT-PCR was performed for key SASP catabolic factors, MMP-1, MMP-3, IL-6, IL-8, ADAMTS-4, ADAMTS-5, TIMP-1, and TIMP-3. mRNA levels of MMP-1 (23-fold, p=0.01921), MMP-3 (20-fold), IL-6 (6-fold), IL-8 (9-fold) were higher in senescent disc cells while ADAMTS4 (1.01-fold), ADAMTS5 (0.93-fold), TIMP1 (1.7-fold), TIMP3 (1.6-fold) remained relatively unchanged compared to control hNP cells (Figure 27). Only the MMPs were transcriptionally upregulated in senescent disc cells while ADAMTS mRNA levels remained relatively unchanged compared to untreated, non-senescent control cells.
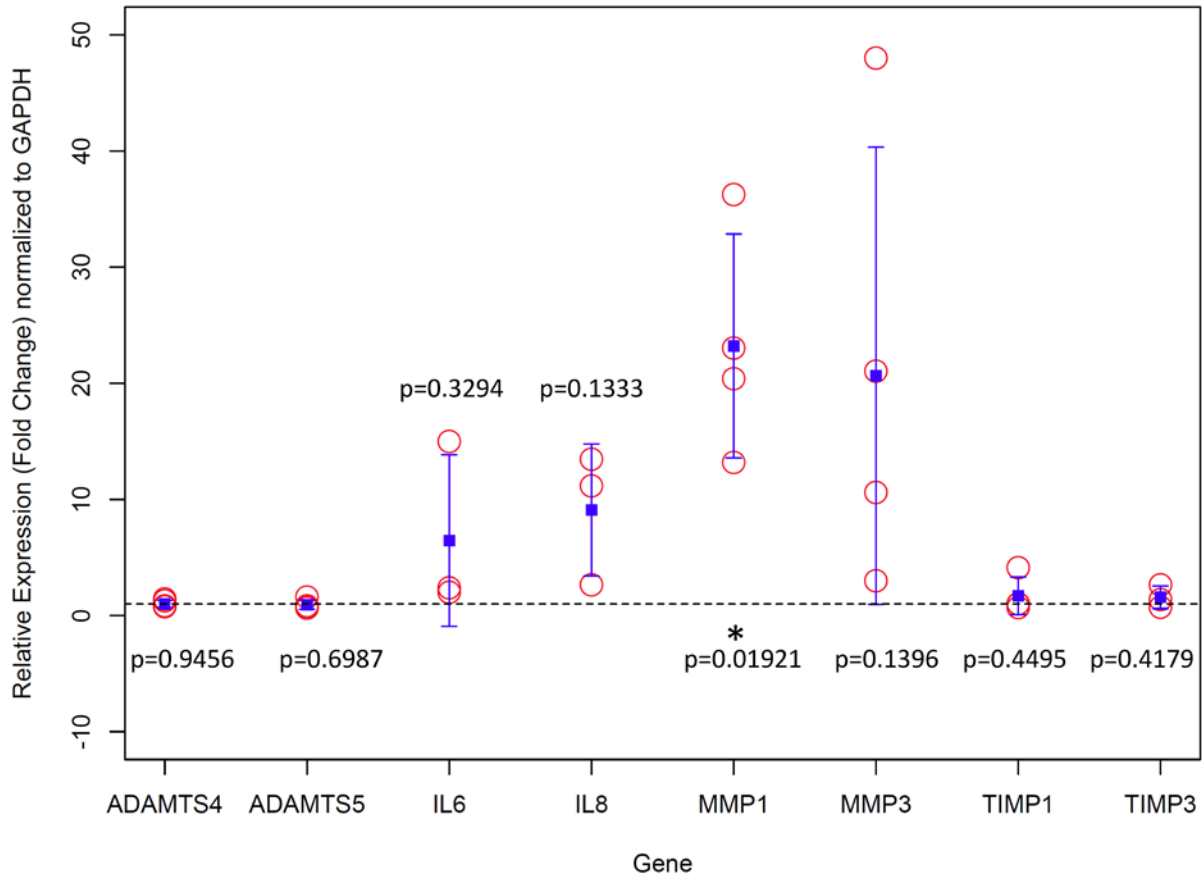
Compared to non-senescent disc cells, senescent disc cells greatly up-regulated mRNA expression of MMP-1, MMP-3, IL-6 and IL-8. Dotted line represents ratio of 1 denoting no change. Blue square represents mean. Error bars represent SEM (n=4).

Figure 27. Oxidative stress-induced senescent hNP cells enhanced expression of catabolic factors.

4.3.2   ELISA for Catabolic Factors

To assess the protein levels of the most upregulated catabolic factors, ELISA was performed for IL-6, IL-8, MMP-1, and MMP-3 in the conditioned media of senescent and non-senescent control hNP cell cultures. Similar to their mRNA expression, MMP-1 (p = 0.008516) and MMP-3 proteins (p = 0.0145) had the greatest increases in secretion from senescent hNP cells compared to control cells with 0.02 pg/mL per cell for senescent compared to undetectable for control for MMP-1 and 0.8 pg/mL per cell (normalized to cell number) for senescent cell media compared to 0.01 pg/mL per cell for control media for MMP-3 (Figure 28). This result supports the hypothesis of Specific Aim 2 that senescent cells secreted increased levels of catabolic factors.
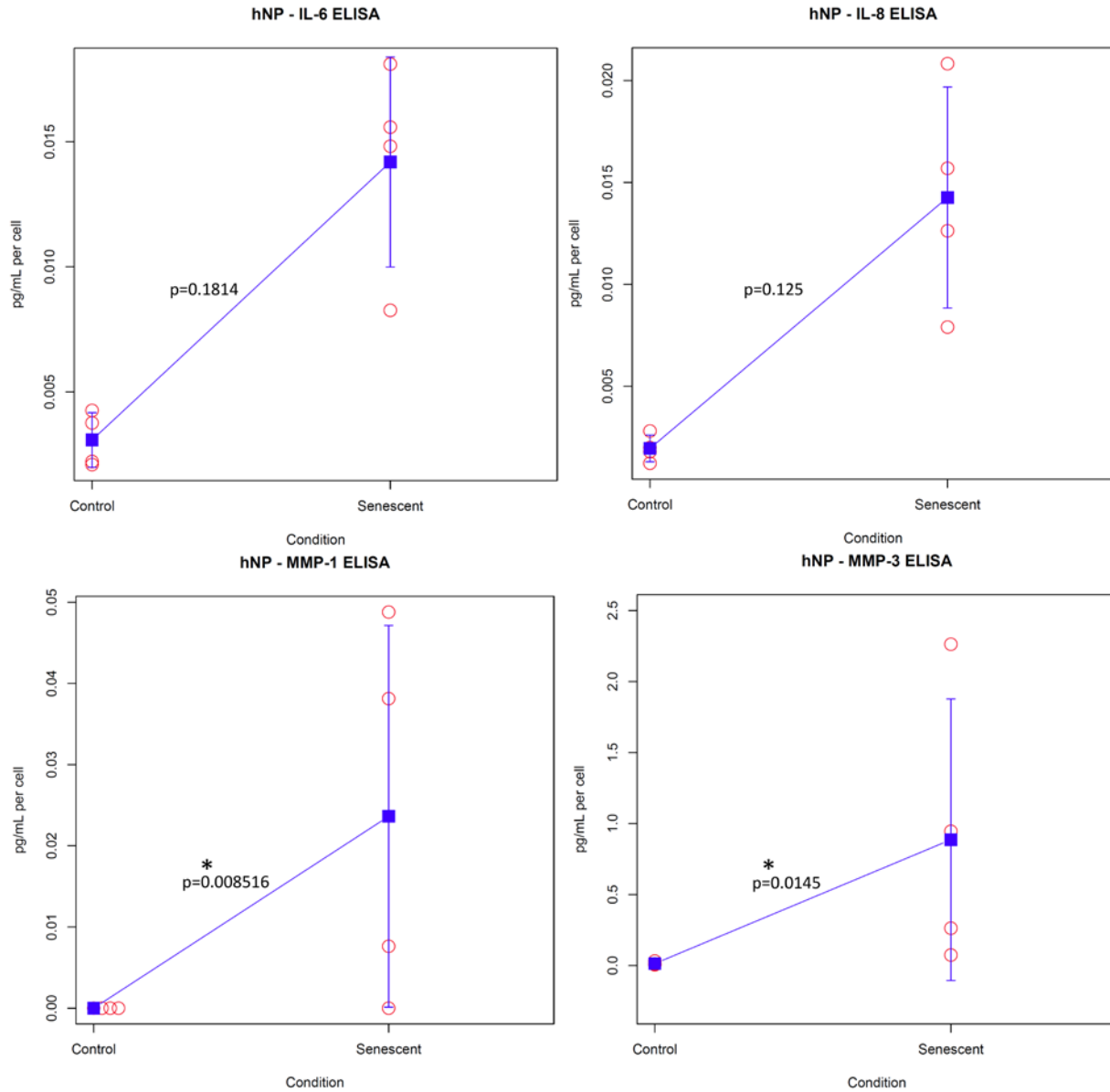
Compared to non-senescent disc (hNP) cells, senescent disc cells greatly increased secretion of catabolic proteins MMP-1, MMP-3, IL-6 and IL-8. Blue square represents mean. Error bars represent SEM (n=4).
Figure 28. Oxidative stress-induced senescent disc cells secrete catabolic factors.

4.3.3   Western Blot for Detection of Aggrecan

To determine whether senescent disc cells produce intact or fragmented aggrecan matrix,

Western blot was performed. Western analysis revealed greater levels of ADAMTS-generated

(Figure 29B) and relatively unchanged MMP-generated (Figure 29C) proteolytic aggrecan

fragments as a result of cleavage in the aggrecan interglobular domain (IGD) in the conditioned

culture media of H_2O_2–induced senescent hNP cells compared to those of nonsenescent hNP

cells. In contrast, the levels of aggrecan IGD proteolytic fragments were relatively unchanged in

the conditioned media of senescent hAF cell culture compared to nonsenescent AF cell culture

(Figure 29).
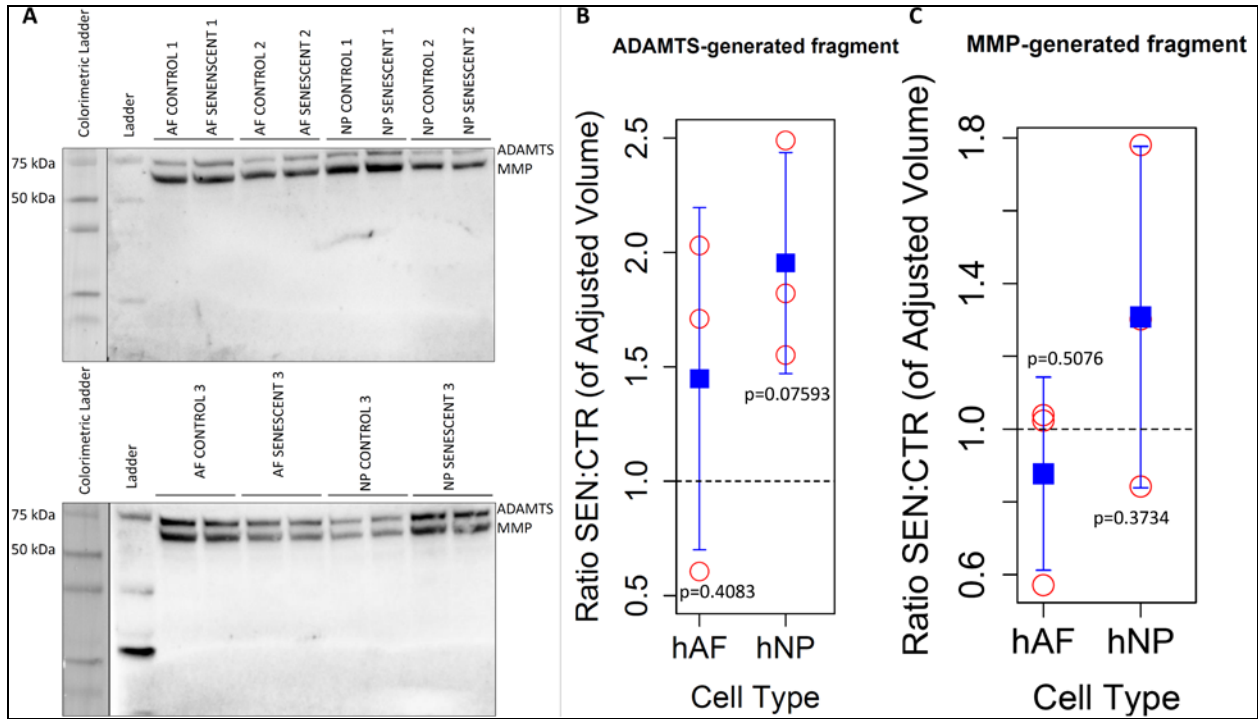
(A)Western blot for detection of Aggrecan (Anti-Agc) in hAF and hNP senescent and negative control conditioned media samples. ADAMTS-generated and MMP-generated fragments indicated. (B) and (C) Quantification of (A) using densitometry represented as relative ratio of volumes for senescent to control CM. Dotted line represents ratio of 1 denoting no change. Blue square represents mean. Error bars represent SEM (n=3).

Figure 29. Oxidative stress-induced senescent disc cells produced more ADAMTS-generated aggrecan fragments.

4.3.4 Inflammation and MMP Antibody Arrays

To assess the secretome profile of senescent disc cells, inflammation and MMP arrays were performed on the conditioned media of senescent and non-senescent control hNP cell cultures. Inflammation (Figure 30B) and MMP (Figure 30A) antibody arrays showed elevated levels of many pro-inflammatory cytokines (IL-6, IL-8, PDGF-BB, GCSF), chemokines (EOTAXIN-2, IP-10, RANTES) and MMPs (MMP-3, MMP-10, TIMP-2) in the conditioned media of senescent hNP cells. Intriguingly, MMP-1 was secreted more from senescent cells as detected by ELISA, however this increase was not detected by the MMP antibody array perhaps indicating lack of sensitivity of the antibody array compared to ELISA. Another possibility for this inconsistency may be the variation between samples isolated from patients with variable age, sex, diagnosis, and degeneration grade.
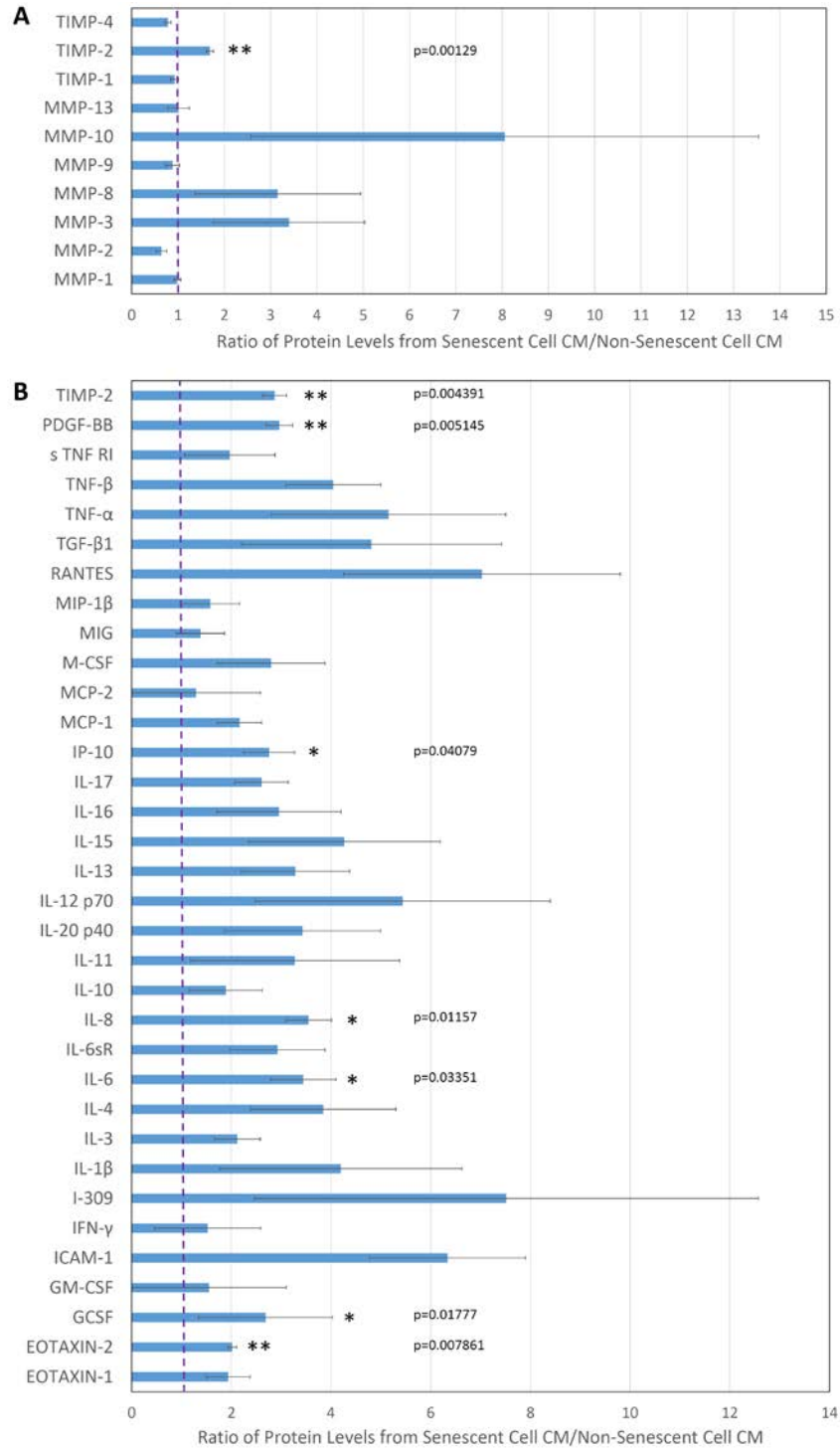
(A) MMP and (B) Inflammation arrays. Error bars represent SEM (n=4). Significance Codes: '**' 0.01 '*' 0.05
Figure 30. Quantified MMP and Inflammation secreted proteins levels are increased in oxidative-stress induced senescent human NP cells.

66

4.3.5   MMP enzymatic activity assay

To evaluate the activity of the MMPs secreted from senescent disc cells, MMP enzymatic activity was performed on conditioned media samples using a fluorogenic substrate. For all samples, there was a lack of MMP enzymatic activity (Figure 31C) from cleavage product fluorescence indicating any trends seen here may only represent changes in noise or background and not meaningful changes between experimental conditions (Figure 31A and 31B). These non-significant changes must be confirmed with modified experimental protocols as these were the initial preliminary experiment for this type of outcome measure. The signal after background subtraction was not strong as it the samples' signals were similar in magnitude to the blank's signal. For samples positive for MMP enzymatic activity, there should be a linear increase in RFU with time with RFU values into the thousands by the last 30 minutes of the assay. However, all samples plateau between 50-100 RFU by the 5 or 10 minute time point (Figure 31C) suggesting a lack of MMP enzymatic activity in all samples. MMPs may have increased mRNA expression and protein secretion; however, there is a lack of MMP enzymatic activity perhaps suggesting post-translational regulation.   For example, the MMPs secreted into conditioned culture media were in the inactive preforms.
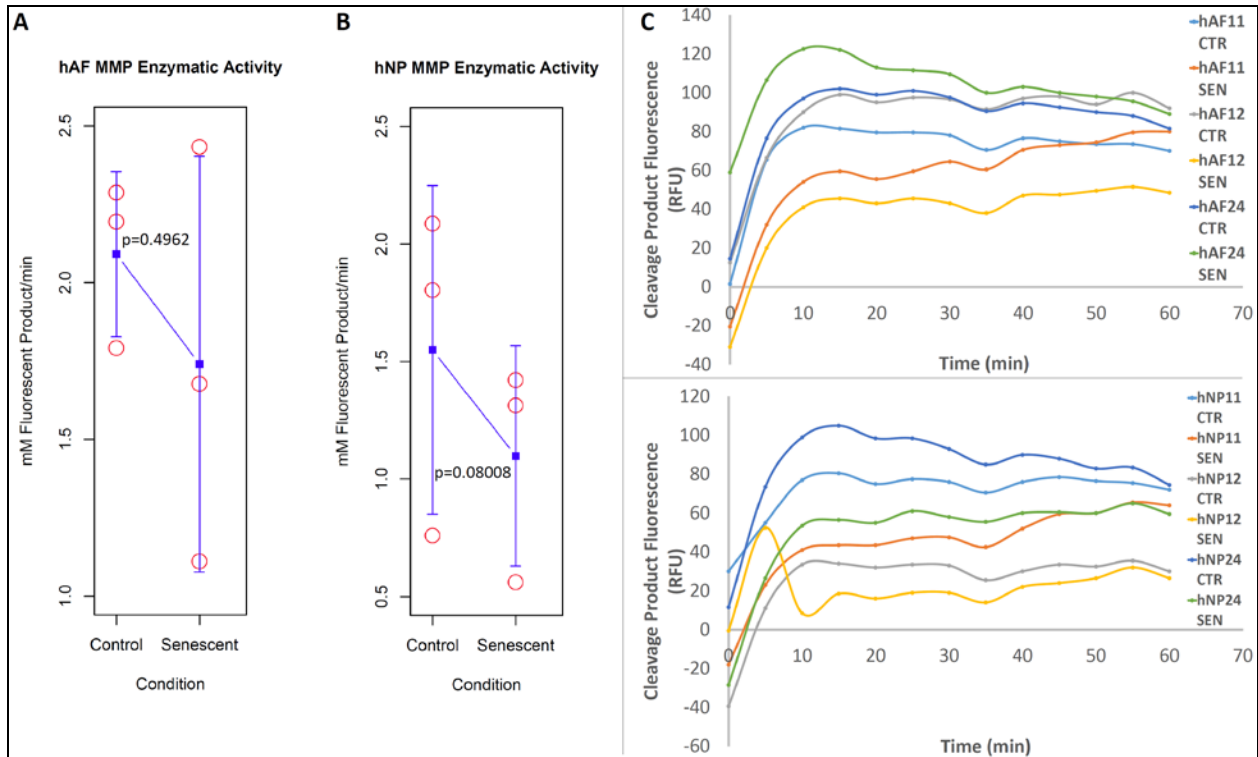
(A) hAF MMP enzymatic activity (mM Fluorescent Product/min). (B) hNP MMP enzymatic activity (mM Fluorescent Product/min). (C) Cleavage Product Fluorescence vs. Time (min). Blue square represents mean. Error bars represent SEM (n=3).

Figure 31. Oxidative-stress induced senescent disc cells display relatively unchanged MMP enzymatic activity.

4.4 TOTAL MATRIX PROTEOGLYCAN CONTENT

4.4.1 GAG (DMMB) Assay

To assess the total GAG content representative of the total PG in hAF and hNP, DMMB assay was performed for senescent and non-senescent control cells. The total GAG content decreased in senescent hAF and hNP cell cultures, the latter was statistically significant while the former was not (Figures 32 and 33).
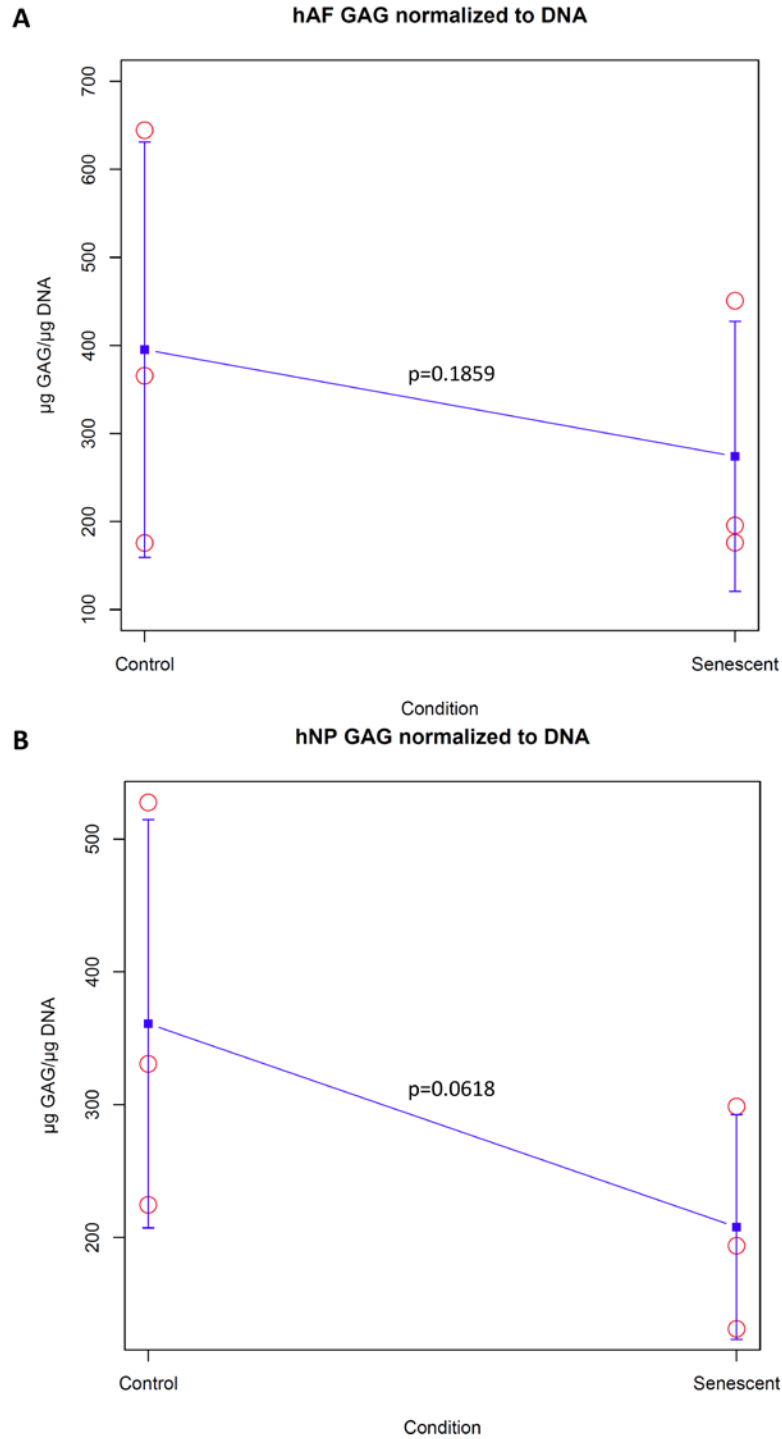
(A) hAF (B) hNP. Normalized to DNA amount. Blue square represents mean. Error bars represent SEM (n=3).
Figure 32. Oxidative-stress induced senescent disc cells display decreased total GAG content.
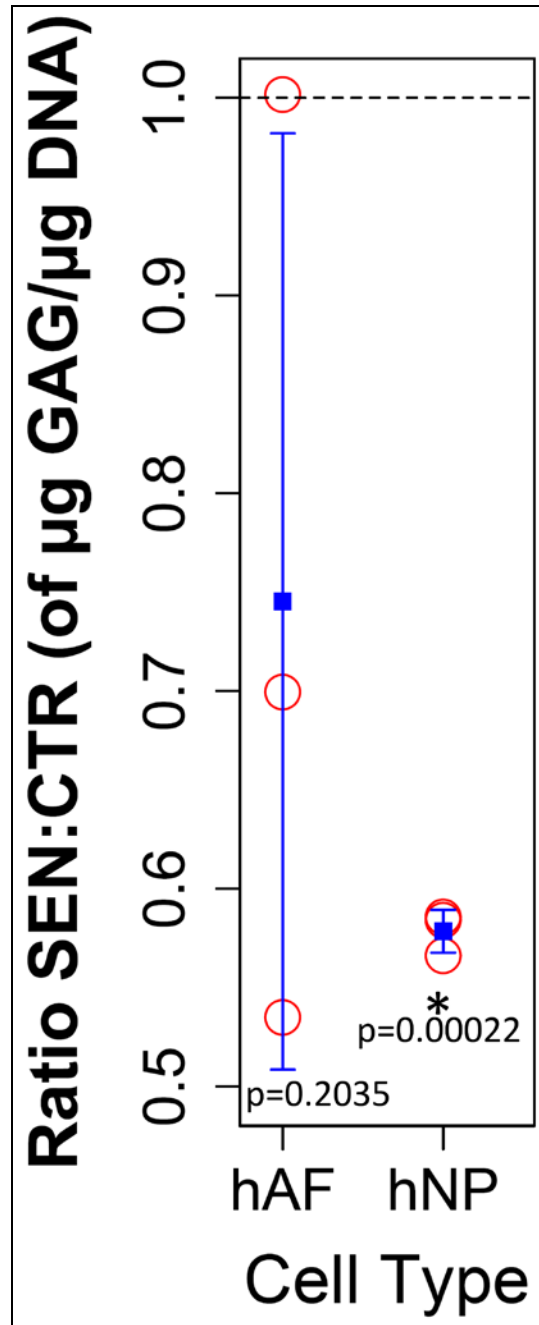
Ratio of Senescent to Control (Total GAG content normalized to DNA). Dotted line represents ratio of 1 denoting no change. Blue square represents mean. Error bars represent SEM (n=3).

Figure 33. Oxidative-stress induced senescent disc cells exhibit a decreased ratio of total GAG content relative to untreated, non-senescent control cells.

5.0   DISCUSSION

5.1   SUMMARY

The goal of my thesis project was to determine if senescent disc cells exhibit perturbed matrix homeostasis. The strong oxidant H_2O_2 was used to induce senescence of human disc cells which showed dramatically perturbed matrix homeostasis, including decreased capacity for new PG synthesis (Figure 25) as well as enhanced expression and secretion of key inflammatory cytokines, chemokines, and matrix proteinases. These are the catabolic factors which constitute the hallmark feature of senescent fibroblasts (Figures 27-28, 30) previously termed senescence associated secretory phenotype (SASP) [47, 84]. Age-dependent accumulation of senescent cells in various organs is thought to disrupt tissue structure and function, and promote aging due at least in part to their SASP. My study showed that stress-induced senescent human disc cells also acquired SASP-like phenotype (Figures 24, 27-28, 30) which may have profound catabolic effects on neighboring cells and the extracellular matrix. Consistent with this idea was the observation of enhanced aggrecanolysis (Figure 29) and decreased total GAG content (Figures 32 and 33) in senescent disc cell culture. Disc senescent cells contribute to perturbed extracellular matrix homeostasis through the acquisition of SASP, reduced matrix synthesis, increased matrix degradation.

5.2   DISC MATRIX ANABOLISM

For anabolism, PG synthesis (Figure 25) and anabolic matrix relative gene expression (Figure 26) were analyzed to detect differences in senescent hAF cells compared to untreated, non-senescent control cells. Senescent cells exhibited a decreasing trend for newly synthesized PG which indicates a reduced capacity of senescent disc cells to produce new matrix to maintain disc matrix homeostasis to offset the process of normal aggrecan turnover. This decreasing trend for PG synthesis also held for hNP for a sample size of 1 patient's donor cells (data not shown). Overall, the PG synthesis results support the hypothesis of decreased anabolism in senescent disc cells for Specific Aim 1.

The major collagen in AF tissue, collagen type I has been shown to express at decreasing levels with age in disc [7]. Decrease in collagen type I expression in senescent hAF cells was consistent with our hypothesis in Specific Aim 1. However, the increase in collagen type II for both hAF and hNP was unexpected as decreased anabolic matrix gene expression was predicted. One possibility is the post-transcriptional or post-translational regulation of collagen type II may differ from collagen type I [85-87]. Perhaps the changes in collagen type I and II expression are merely indicative of there being more collagen in hAF than hNP. The relatively unchanged expression of aggrecan, versican, and link protein is not consistent with the decreased PG synthesis in senescent hAF cells result, implying post-transcriptional and or post-translational regulations [19, 88-93] which account for decreased translation, export, and assembly.

Collagen type I transitions to greater proportions collagen type II from outer AF to inner AF and NP. During early stages of degeneration, the amount of the major collagen types I and II are increased along with the minor types (III, V, VI). During degeneration, the ratio of type I-to-type II collagen increases in the inner AF and NP, which may result from an increase in type I

73

collagen or a decrease in type II collagen [94]. Taking this into consideration when interpreting the decrease in collagen type I and increase in collagen type II for hAF gene expression, this outcome is contradictory to the increasing type I-to-type II collagen ratio in degenerated inner AF and NP and may imply a shift to a more chondrocytic phenotype (more similar to NP). However, the increase in collagen type II mRNA expression in senescent cells compared to control cells in hNP is intriguing and contradictory to my hypothesis as it would be beneficial to the NP function of resisting compressive forces. Further experiments are needed to confirm whether the collagen type I and II protein levels correlate with their mRNA expression levels. If confirmed, this would suggest that the whole disc structure may be less efficient for its native function in resisting tensile strain due to the shift of both the hAF and hNP towards a more collagen type II-rich, chondrocytic phenotype.

5.3   DISC MATRIX CATABOLISM

For hNP senescent cells, expression of SASP factors IL-6, IL-8, MMP-1, MMP-3 [67] were found to be upregulated both at the levels of transcription (Figure 27) as well as protein (Figure 28). The relative mRNA gene expressions of ADAMTS-4 and ADAMTS-5 as well as the catabolic tissue inhibitors TIMP-1 and TIMP-3 in hNP senescent cells did not change much, possibly due to post-translational modulation rather than transcriptional regulation [95-98]. Inflammation and MMP antibody arrays revealed that senescent disc cells secrete many pro-inflammatory cytokines, chemokines, and remodeling factors characteristic of SASP [67, 99]. Overall, the catabolic gene expression, ELISA, and inflammation and MMP antibody array

findings supported the hypothesis of increased catabolism in senescent disc cells proposed in Specific Aim 2.

Western blot for aggrecan (Figure 29) revealed increased ADAMTS-generated aggrecan fragments (Figure 29B) and relatively unchanged MMP-generated aggrecan fragments in senescent disc cell cultures. These results are intriguing because   MMP-1 and MMP-3 mRNA and protein expressions increased in senescent disc cells while ADAMTS-4 and ADAMTS-5 mRNA expression remained unchanged.   It is likely that in cell cultures there may be post-translational regulation influencing the enzymatic activity of the aggrecanases (becoming activated) and MMPs (remaining inactive) [95, 96].   In fact, MMPs are secreted in a latent, inactive pro-form, and my assessment of MMP enzymatic activity showed minimal enzymatic activity in both senescent and control hNP cell conditioned media (Figure 30). This result still seems contradictory to the MMP-generated aggrecan fragments detected by Western blot indicating some enzymatic activity in both senescent and control disc cells conditioned media despite the lack of a difference between conditions. However, TIMP inhibition can confound the results of the MMP enzymatic activity assay as these catabolic inhibitors regulate MMPs and ADAMTSs as has been documented in disc specifically [100-103].   TIMP inhibition may be masking the ability for MMP activity assay to detect any fluorogenic product cleavage from both senescent and control disc cell conditioned media samples. Another possibility for the lack of observed MMP enzymatic activity may be the treatment with 500 µM hydrogen peroxide as greater than 50 µM of ROS has been previously reported to inhibit MMP activity *in vitro* [104-107], however this seems unlikely as the hydrogen peroxide media was removed after two hours and replaced with fresh media. An additional possibility for the lack of MMP activity may be the late stage attenuation of SASP by microRNAs, mir-146a and mir-146b, reported to decrease NF-

κB activity after secretion from senescent cells *in vitro* after IL-6 and IL-8 secretion peaks [47, 48, 99, 108]. Overall, this Western blot finding supported the hypothesis that senescent cells have increased catabolism of disc matrix for Specific Aim 2 while the MMP activity finding does not support this hypothesis. It must be viewed as inconclusive at this time. There may be a basal level of MMP activity for aggrecan proteolysis while MMPs are upregulated in senescent cells in this latent, inactive pro-form such that there was not a higher amount of MMP-generated aggrecan fragments detected in senescent disc cells.

5.4   DISC TOTAL MATRIX PROTEOGLYCAN CONTENT

Total PG matrix content was measured using the DMMB assay for GAG.   There was a significant decrease in total GAG content from senescent hNP cells compared to non-senescent control cells (Figures 32 and 33). The net GAG content was determined by matrix homeostatic balance, i.e., rates of catabolism vs anabolism. My anabolic and catabolic findings along with this decreased total GAG content of the disc matrix supports the idea that senescent disc cells acquire an imbalance of disc matrix homeostasis. Overall the findings support the central hypothesis of decreased anabolism and increased catabolism in senescent disc cells.

5.5   LIMITATIONS

One of the biggest limitations in the disc field is the lack of fresh control specimens from healthy human donors to compare with degenerated discs. The disc specimens isolated from surgeries on individuals with low back pain are likely degenerative. Also, the frequency of human disc specimen availability, amount of disc tissue and cells isolated from those tissues, and the generally slower growth rate than healthy animal models (rabbits, cows…) provides unique challenges to studying the disc in human. Another caveat is the growth condition. Naturally, the disc cells reside in a low oxygen environment, and thus culture of disc cells at atmospheric oxygen (20%) in normal incubators is not ideal. However, this is often done in the disc field due to cost constraint.   Recently, disc cell culture research in my laboratory is moving toward using hypoxic chambers to better mimic the physiological condition of disc tissue. More specifically to this study, human specimens from patients are widely variable due to the inability to match for age, sex, degeneration grade without a large pool of donors to choose from. This variability between donors generally translates to high variances between samples for all outcome measures. The small sample size is quite limiting for statistical power such that a sample size of 5 or 6 is required to see any significant change for such variable samples.

The next limitation would be the monolayer cell culture that all these experiments were performed in. Our lab utilized 3D cell cultures with alginates beads primarily for rabbit NP cell as the large cell numbers needed for enough beads for experiments is attainable for rabbit, but not as easily for human degenerated samples. Disc cells better retain their phenotype when in 3D culture compared to monolayer as 3D is more similar to their native environment.

These disc primary cells are further limited in that their phenotype begins to shift by passage 3 thus proliferation and expansion is limited for primary cells from each donor constraining the amount of experiments that can be performed.

5.6   FUTURE DIRECTIONS

A stress control should also be performed to compare ER stress via drugs like thapsigargin, tunicamycin, bortezomid, and cyclosporine in order to compare to the mitochondrial stress of H_2O_2 to confirm these results are specific to oxidative stress rather than stress in general. This may be monitored with gene expression of Xbp1 (spliced variant) and C/EBP Homologous Protein (CHOP) via qRT-PCR to differentiate H_2O_2 (mitochondrial) stress response from other stress responses (ER stress).

For current experiments, further work will increase the sample size of outcome measures such as PG synthesis, anabolic PCR, total GAG content, western for aggrecan proteolysis to further corroborate the findings observed so far. Western blot for ADAMTS-4 and ADAMTS-5 in conditioned media from senescent and non-senescent cell is needed to further elucidate the specific ADAMTS is primarily responsible for the proteolytic cleavage of aggrecan in the disc matrix. Western blot will also be performed on conditioned media for TIMPs such as TIMP-1, TIMP-2, and TIMP-3 for comparison of these protein levels secreted from senescent disc cells and control cells. TIMP inhibition assay quenched fluorescent substrate assay) should also be performed to determine the amount of inhibition in a conditioned media sample to further elucidate the lack of MMP activity in the senescent cell conditioned media samples.

To further examine the changes in collagen type I and II metabolism in senescent disc cells, collagen synthesis with radiolabeled proline (^{3}H-L-Proline) will be performed and compared to the PG synthesis findings. Also, to corroborate the decrease of collagen type I in hAF and increase in collagen type II in hAF and hNP samples, anti-collagen antibodies can be used to assay collagen degradation [109, 110] as well as more qRT-PCR to increase the sample size. The expected outcomes would be decreased collagen synthesis and increased collagen degradation generated in senescent disc cells compared to non-senescent control cells.

Future *in vivo* experiments are needed to assess similar outcome measures as performed in this in vitro study from the discs from an accelerated aging (progeroid) mouse model compared to old and young wild type mice to confirm the role of disc cellular senescence in matrix homeostatic imbalance. More important, *in vivo* studies are also needed to investigate whether clearance of senescent cells in accelerated aging mice or naturally aging mice [71] affects disc tissue structure and function.

6.0   PUBLIC HEALTH SIGNIFICANCE

By 2050, the world population is estimated to have 1.5 billion of individuals ages 65 and older compared to 524 million in 2010 [32, 33]. Aging is the largest single risk factor for intervertebral disc degeneration (IDD), as disc matrix proteoglycan (PG) is invariably and progressively depleted with age [76]. Dysregulated disc cells are thought to drive age-associated disc PG loss through a combination of reduced capacity to synthesize matrix PG and increased production of proteolytic enzymes to breakdown matrix [111]. The link between aged degenerative discs and cellular senescence has been previously observed in human discs [74, 75], but it remains unknown if senescent disc cells are phenotypically different from their non-senescent counterpart in terms of matrix homeostasis.

How aging disrupts disc matrix homeostasis leading to PG loss and IDD is not clearly understood. Implicating cellular senescence (and SASP development) as a driver of disc PG loss and IDD will offer novel opportunities for targeted therapy to prevent or treat IDD, which would have a tremendous public health impact in preventing or limiting chronic low back pain.

Hence, understanding the biology of disc aging is critical in developing effective therapeutic interventions to treat age-related IDD disorders. This is imperative because of the growing aging population which is expected to bring great burdens and challenges from the many age-related diseases. This thesis research initiated and established a basic framework of how aging affects disc health through the action of senescent disc cells on matrix metabolism.

BIBLIOGRAPHY

1. Roughley PJ. 2004. *Biology of intervertebral disc aging and degeneration: involvement of the extracellular matrix*. Spine **29:**2691-2699.
2. Huang YC, Urban JP, Luk KD. 2014. *Intervertebral disc regeneration: do nutrients lead the way?* Nature reviews. Rheumatology.
3. Urban JP, Roberts S. 2003. *Degeneration of the intervertebral disc*. Arthritis research & therapy **5:**120-130.
4. Maroudas A, Stockwell RA, Nachemson A, Urban J. 1975. *Factors involved in the nutrition of the human lumbar intervertebral disc: cellularity and diffusion of glucose in vitro*. Journal of anatomy **120:**113-130.
5. Marchand F, Ahmed AM. 1990. *Investigation of the laminate structure of lumbar disc anulus fibrosus*. Spine **15:**402-410.
6. Setton L BL, Masuda K. *Regeneration and Replacement of the Intervertebral Disc*, 3 ed. Elsevier Press.
7. Cho H, Park SH, Lee S, Kang M, Hasty KA, Kim SJ. 2011. *Snapshot of degenerative aging of porcine intervertebral disc: a model to unravel the molecular mechanisms*. Experimental & molecular medicine **43:**334-340.
8. Adams MA, Roughley PJ. 2006. *What is intervertebral disc degeneration, and what causes it?* Spine **31:**2151-2161.
9. Roberts S, Urban JPG. 2011. *Intervertebral Discs*. *In* Stellman JM (ed.), Encyclopedia of Occupational Health and Safety. International Labor Organization, Geneva.
10. Visse R, Nagase H. 2003. *Matrix metalloproteinases and tissue inhibitors of metalloproteinases: structure, function, and biochemistry*. Circulation research **92:**827-839.
11. Mott JD, Werb Z. 2004. *Regulation of matrix biology by matrix metalloproteinases*. Current opinion in cell biology **16:**558-564.
12. Duffy MJ, Lynn DJ, Lloyd AT, O'Shea CM. 2003. *The ADAMs family of proteins: from basic studies to potential clinical applications*. Thrombosis and haemostasis **89:**622-631.
13. Tang BL. 2001. *ADAMTS: a novel family of extracellular matrix proteases*. The international journal of biochemistry & cell biology **33:**33-44.
14. Porter S, Clark IM, Kevorkian L, Edwards DR. 2005. *The ADAMTS metalloproteinases*. The Biochemical journal **386:**15-27.
15. Roberts S, Caterson B, Menage J, Evans EH, Jaffray DC, Eisenstein SM. 2000. *Matrix metalloproteinases and aggrecanase: their role in disorders of the human intervertebral disc*. Spine **25:**3005-3013.
16. Goupille P, Jayson MI, Valat JP, Freemont AJ. 1998. *Matrix metalloproteinases: the clue to intervertebral disc degeneration?* Spine **23:**1612-1626.

17. Antoniou J, Steffen T, Nelson F, Winterbottom N, Hollander AP, Poole RA, Aebi M, Alini M. 1996. *The human lumbar intervertebral disc: evidence for changes in the biosynthesis and denaturation of the extracellular matrix with growth, maturation, ageing, and degeneration*. The Journal of clinical investigation **98:**996-1003.

18. Adams MA, Hutton WC. 1982. *Prolapsed intervertebral disc. A hyperflexion injury 1981 Volvo Award in Basic Science*. Spine **7:**184-191.

19. Nagase H, Kashiwagi M. 2003. *Aggrecanases and cartilage matrix degradation*. Arthritis research & therapy **5:**94-103.

20. Sivan SS, Wachtel E, Roughley P. 2014. *Structure, function, aging and turnover of aggrecan in the intervertebral disc*. Biochimica et biophysica acta.

21. Urban JP, Smith S, Fairbank JC. 2004. *Nutrition of the intervertebral disc*. Spine **29:**2700-2709.

22. Gregory DS, Seto CK, Wortley GC, Shugart CM. 2008. *Acute lumbar disk pain: navigating evaluation and treatment choices*. American family physician **78:**835-842.

23. van Tulder MW, Scholten RJ, Koes BW, Deyo RA. 2000. *Non-steroidal anti-inflammatory drugs for low back pain*. The Cochrane database of systematic reviews**:**CD000396.

24. van Tulder MW, Touray T, Furlan AD, Solway S, Bouter LM, Cochrane Back Review G. 2003. *Muscle relaxants for nonspecific low back pain: a systematic review within the framework of the cochrane collaboration*. Spine **28:**1978-1992.

25. Luijsterburg PA, Verhagen AP, Ostelo RW, van Os TA, Peul WC, Koes BW. 2007. *Effectiveness of conservative treatments for the lumbosacral radicular syndrome: a systematic review*. European spine journal : official publication of the European Spine Society, the European Spinal Deformity Society, and the European Section of the Cervical Spine Research Society **16:**881-899.

26. Luijsterburg PA, Lamers LM, Verhagen AP, Ostelo RW, van den Hoogen HJ, Peul WC, Avezaat CJ, Koes BW. 2007. *Cost-effectiveness of physical therapy and general practitioner care for sciatica*. Spine **32:**1942-1948.

27. Hagen KB, Hilde G, Jamtvedt G, Winnem M. 2000. *Bed rest for acute low back pain and sciatica*. The Cochrane database of systematic reviews**:**CD001254.

28. Saal JA, Saal JS. 1989. *Nonoperative treatment of herniated lumbar intervertebral disc with radiculopathy. An outcome study*. Spine **14:**431-437.

29. Grunhagen T, Shirazi-Adl A, Fairbank JC, Urban JP. 2011. *Intervertebral disk nutrition: a review of factors influencing concentrations of nutrients and metabolites*. The Orthopedic clinics of North America **42:**465-477, vii.

30. Sivan SS, Hayes AJ, Wachtel E, Caterson B, Merkher Y, Maroudas A, Brown S, Roberts S. 2014. *Biochemical composition and turnover of the extracellular matrix of the normal and degenerate intervertebral disc*. European spine journal : official publication of the European Spine Society, the European Spinal Deformity Society, and the European Section of the Cervical Spine Research Society **23 Suppl 3:**344-353.

31. Stefanovic-Racic M, Stadler J, Georgescu HI, Evans CH. 1994. *Nitric oxide and energy production in articular chondrocytes*. Journal of cellular physiology **159:**274-280.

32. Risbud MV, Shapiro IM. 2014. *Role of cytokines in intervertebral disc degeneration: pain and disc content*. Nature reviews. Rheumatology **10:**44-56.

33. Andersson GB. 1999. *Epidemiological features of chronic low-back pain*. Lancet **354:**581-585.

34. Rubin DI. 2007. *Epidemiology and risk factors for spine pain*. Neurologic clinics **25:**353-371.

35. Deyo RA, Weinstein JN. 2001. *Low back pain*. The New England journal of medicine **344:**363-370.

36. Dagenais S, Caro J, Haldeman S. 2008. *A systematic review of low back pain cost of illness studies in the United States and internationally*. The spine journal : official journal of the North American Spine Society **8:**8-20.

37. Boos N, Weissbach S, Rohrbach H, Weiler C, Spratt KF, Nerlich AG. 2002. *Classification of age-related changes in lumbar intervertebral discs: 2002 Volvo Award in basic science*. Spine **27:**2631-2644.

38. Haefeli M, Kalberer F, Saegesser D, Nerlich AG, Boos N, Paesold G. 2006. *The course of macroscopic degeneration in the human lumbar intervertebral disc*. Spine **31:**1522-1531.

39. Suzman R, Beard J. 2014. *Global Health and Aging*. National Institute of Aging.

40. Tchkonia T, Zhu Y, van Deursen J, Campisi J, Kirkland JL. 2013. *Cellular senescence and the senescent secretory phenotype: therapeutic opportunities*. The Journal of clinical investigation **123:**966-972.

41. Munoz-Espin D, Serrano M. 2014. *Cellular senescence: from physiology to pathology*. Nature reviews. Molecular cell biology **15:**482-496.

42. Chicas A, Wang X, Zhang C, McCurrach M, Zhao Z, Mert O, Dickins RA, Narita M, Zhang M, Lowe SW. 2010. *Dissecting the unique role of the retinoblastoma tumor suppressor during cellular senescence*. Cancer cell **17:**376-387.

43. Perez-Mancera PA, Young AR, Narita M. 2014. *Inside and out: the activities of senescence in cancer*. Nature reviews. Cancer **14:**547-558.

44. Harley CB, Futcher AB, Greider CW. 1990. *Telomeres shorten during ageing of human fibroblasts*. Nature **345:**458-460.

45. d'Adda di Fagagna F, Reaper PM, Clay-Farrace L, Fiegler H, Carr P, Von Zglinicki T, Saretzki G, Carter NP, Jackson SP. 2003. *A DNA damage checkpoint response in telomere-initiated senescence*. Nature **426:**194-198.

46. Herbig U, Jobling WA, Chen BP, Chen DJ, Sedivy JM. 2004. *Telomere shortening triggers senescence of human cells through a pathway involving ATM, p53, and p21(CIP1), but not p16(INK4a)*. Molecular cell **14:**501-513.

47. Rodier F, Campisi J. 2011. *Four faces of cellular senescence*. The Journal of cell biology **192:**547-556.

48. Bhaumik D, Scott GK, Schokrpur S, Patil CK, Orjalo AV, Rodier F, Lithgow GJ, Campisi J. 2009. *MicroRNAs miR-146a/b negatively modulate the senescence-associated inflammatory mediators IL-6 and IL-8*. Aging **1:**402-411.

49. McShea A, Harris PL, Webster KR, Wahl AF, Smith MA. 1997. *Abnormal expression of the cell cycle regulators P16 and CDK4 in Alzheimer's disease*. The American journal of pathology **150:**1933-1939.

50. Hebert LE, Scherr PA, Bienias JL, Bennett DA, Evans DA. 2003. *Alzheimer disease in the US population: prevalence estimates using the 2000 census*. Archives of neurology **60:**1119-1122.

51. Cohen G. 1983. *The pathobiology of Parkinson's disease: biochemical aspects of dopamine neuron senescence*. Journal of neural transmission. Supplementum **19:**89-103.

52. Liton PB, Challa P, Stinnett S, Luna C, Epstein DL, Gonzalez P. 2005. *Cellular senescence in the glaucomatous outflow pathway*. Experimental gerontology **40:**745-748.
53. Minamino T, Miyauchi H, Yoshida T, Ishida Y, Yoshida H, Komuro I. 2002. *Endothelial cell senescence in human atherosclerosis: role of telomere in endothelial dysfunction*. Circulation **105:**1541-1544.
54. Holdt LM, Sass K, Gabel G, Bergert H, Thiery J, Teupser D. 2011. *Expression of Chr9p21 genes CDKN2B (p15(INK4b)), CDKN2A (p16(INK4a), p14(ARF)) and MTAP in human atherosclerotic plaque*. Atherosclerosis **214:**264-270.
55. Krishnamurthy J, Torrice C, Ramsey MR, Kovalev GI, Al-Regaiey K, Su L, Sharpless NE. 2004. *Ink4a/Arf expression is a biomarker of aging*. The Journal of clinical investigation **114:**1299-1307.
56. Aoshiba K, Nagai A. 2009. *Senescence hypothesis for the pathogenetic mechanism of chronic obstructive pulmonary disease*. Proceedings of the American Thoracic Society **6:**596-601.
57. Kirzner Y, Marcolongo M, Bhatia SK. 2012. *Advances in biomaterials for the treatment of intervertebral disc degeneration*. Journal of long-term effects of medical implants **22:**73-84.
58. Tsuji T, Aoshiba K, Nagai A. 2004. *Cigarette smoke induces senescence in alveolar epithelial cells*. American journal of respiratory cell and molecular biology **31:**643-649.
59. Loeser RF. 2009. *Aging and osteoarthritis: the role of chondrocyte senescence and aging changes in the cartilage matrix*. Osteoarthritis and cartilage / OARS, Osteoarthritis Research Society **17:**971-979.
60. Martin JA, Brown T, Heiner A, Buckwalter JA. 2004. *Post-traumatic osteoarthritis: the role of accelerated chondrocyte senescence*. Biorheology **41:**479-491.
61. Martin JA, Buckwalter JA. 2003. *The role of chondrocyte senescence in the pathogenesis of osteoarthritis and in limiting cartilage repair*. The Journal of bone and joint surgery. American volume **85-A Suppl 2:**106-110.
62. Price JS, Waters JG, Darrah C, Pennington C, Edwards DR, Donell ST, Clark IM. 2002. *The role of chondrocyte senescence in osteoarthritis*. Aging cell **1:**57-65.
63. Minamino T, Orimo M, Shimizu I, Kunieda T, Yokoyama M, Ito T, Nojima A, Nabetani A, Oike Y, Matsubara H, Ishikawa F, Komuro I. 2009. *A crucial role for adipose tissue p53 in the regulation of insulin resistance*. Nature medicine **15:**1082-1087.
64. Tchkonia T, Morbeck DE, Von Zglinicki T, Van Deursen J, Lustgarten J, Scrable H, Khosla S, Jensen MD, Kirkland JL. 2010. *Fat tissue, aging, and cellular senescence*. Aging cell **9:**667-684.
65. Kang TW, Yevsa T, Woller N, Hoenicke L, Wuestefeld T, Dauch D, Hohmeyer A, Gereke M, Rudalska R, Potapova A, Iken M, Vucur M, Weiss S, Heikenwalder M, Khan S, Gil J, Bruder D, Manns M, Schirmacher P, Tacke F, Ott M, Luedde T, Longerich T, Kubicka S, Zender L. 2011. *Senescence surveillance of pre-malignant hepatocytes limits liver cancer development*. Nature **479:**547-551.
66. Xue W, Zender L, Miething C, Dickins RA, Hernando E, Krizhanovsky V, Cordon-Cardo C, Lowe SW. 2007. *Senescence and tumour clearance is triggered by p53 restoration in murine liver carcinomas*. Nature **445:**656-660.
67. Freund A, Patil CK, Campisi J. 2011. *p38MAPK is a novel DNA damage response-independent regulator of the senescence-associated secretory phenotype*. The EMBO journal **30:**1536-1548.

68. Naylor RM, Baker DJ, van Deursen JM. 2013. *Senescent cells: a novel therapeutic target for aging and age-related diseases*. Clinical pharmacology and therapeutics **93:**105-116.

69. Wang W, Wu J, Zhang Z, Tong T. 2001. *Characterization of regulatory elements on the promoter region of p16(INK4a) that contribute to overexpression of p16 in senescent fibroblasts*. The Journal of biological chemistry **276:**48655-48661.

70. Pajvani UB, Trujillo ME, Combs TP, Iyengar P, Jelicks L, Roth KA, Kitsis RN, Scherer PE. 2005. *Fat apoptosis through targeted activation of caspase 8: a new mouse model of inducible and reversible lipoatrophy*. Nature medicine **11:**797-803.

71. Baker DJ, Wijshake T, Tchkonia T, LeBrasseur NK, Childs BG, van de Sluis B, Kirkland JL, van Deursen JM. 2011. *Clearance of p16Ink4a-positive senescent cells delays ageing-associated disorders*. Nature **479:**232-236.

72. Strindhall J, Nilsson BO, Lofgren S, Ernerudh J, Pawelec G, Johansson B, Wikby A. 2007. *No Immune Risk Profile among individuals who reach 100 years of age: findings from the Swedish NONA immune longitudinal study*. Experimental gerontology **42:**753-761.

73. Franceschi C, Capri M, Monti D, Giunta S, Olivieri F, Sevini F, Panourgia MP, Invidia L, Celani L, Scurti M, Cevenini E, Castellani GC, Salvioli S. 2007. *Inflammaging and anti-inflammaging: a systemic perspective on aging and longevity emerged from studies in humans*. Mechanisms of ageing and development **128:**92-105.

74. Le Maitre CL, Freemont AJ, Hoyland JA. 2007. *Accelerated cellular senescence in degenerate intervertebral discs: a possible role in the pathogenesis of intervertebral disc degeneration*. Arthritis research & therapy **9:**R45.

75. Gruber HE, Ingram JA, Davis DE, Hanley EN, Jr. 2009. *Increased cell senescence is associated with decreased cell proliferation in vivo in the degenerating human annulus*. The spine journal : official journal of the North American Spine Society **9:**210-215.

76. Miller JA, Schmatz C, Schultz AB. 1988. *Lumbar disc degeneration: correlation with age, sex, and spine level in 600 autopsy specimens*. Spine **13:**173-178.

77. Chen JH OS, Hales CN. 2007. *Methods of cellular senescence induction using oxidative stress*. Methods in molecular biology**:**178-189.

78. Dimri GP, Lee X, Basile G, Acosta M, Scott G, Roskelley C, Medrano EE, Linskens M, Rubelj I, Pereira-Smith O, et al. 1995. *A biomarker that identifies senescent human cells in culture and in aging skin in vivo*. Proceedings of the National Academy of Sciences of the United States of America **92:**9363-9367.

79. Wang D, Vo NV, Sowa GA, Hartman RA, Ngo K, Choe SR, Witt WT, Dong Q, Lee JY, Niedernhofer LJ, Kang JD. 2011. *Bupivacaine decreases cell viability and matrix protein synthesis in an intervertebral disc organ model system*. The spine journal : official journal of the North American Spine Society **11:**139-146.

80. Vo N, Wang D, Sowa G, Witt W, Ngo K, Coelho P, Bedison R, Byer B, Studer R, Lee J, Di YP, Kang J. 2011. *Differential effects of nicotine and tobacco smoke condensate on human annulus fibrosus cell metabolism*. Journal of orthopaedic research : official publication of the Orthopaedic Research Society **29:**1585-1591.

81. Studer RK, Vo N, Sowa G, Ondeck C, Kang J. 2011. *Human nucleus pulposus cells react to IL-6: independent actions and amplification of response to IL-1 and TNF-alpha*. Spine **36:**593-599.

82. Livak KJ, Schmittgen TD. 2001. *Analysis of relative gene expression data using real-time quantitative PCR and the 2(-Delta Delta C(T)) Method*. Methods **25:**402-408.

83. Fields GB. 2010. *Using fluorogenic peptide substrates to assay matrix metalloproteinases*. Methods in molecular biology **622:**393-433.
84. Campisi J, d'Adda di Fagagna F. 2007. *Cellular senescence: when bad things happen to good cells*. Nature reviews. Molecular cell biology **8:**729-740.
85. Kay EP, He YG. 1991. *Post-transcriptional and transcriptional control of collagen gene expression in normal and modulated rabbit corneal endothelial cells*. Investigative ophthalmology & visual science **32:**1821-1827.
86. Yamauchi M, Sricholpech M. 2012. *Lysine post-translational modifications of collagen*. Essays in biochemistry **52:**113-133.
87. Pokidysheva E, Zientek KD, Ishikawa Y, Mizuno K, Vranka JA, Montgomery NT, Keene DR, Kawaguchi T, Okuyama K, Bachinger HP. 2013. *Posttranslational modifications in type I collagen from different tissues extracted from wild type and prolyl 3-hydroxylase 1 null mice*. The Journal of biological chemistry **288:**24742-24752.
88. Tammi RH, Passi AG, Rilla K, Karousou E, Vigetti D, Makkonen K, Tammi MI. 2011. *Transcriptional and post-translational regulation of hyaluronan synthesis*. The FEBS journal **278:**1419-1428.
89. Thiebot B, Langris M, Bonnamy PJ, Bocquet J. 1998. *Regulation of proteoglycan and hyaluronan synthesis by elevated level of intracellular cyclic adenosine monophosphate in peritubular cells from immature rat testis*. Molecular and cellular biochemistry **187:**99-112.
90. Fischer JW, Schror K. 2007. *Regulation of hyaluronan synthesis by vasodilatory prostaglandins. Implications for atherosclerosis*. Thrombosis and haemostasis **98:**287-295.
91. Li L, Asteriou T, Bernert B, Heldin CH, Heldin P. 2007. *Growth factor regulation of hyaluronan synthesis and degradation in human dermal fibroblasts: importance of hyaluronan for the mitogenic response of PDGF-BB*. The Biochemical journal **404:**327-336.
92. Jokela TA, Jauhiainen M, Auriola S, Kauhanen M, Tiihonen R, Tammi MI, Tammi RH. 2008. *Mannose inhibits hyaluronan synthesis by down-regulation of the cellular pool of UDP-N-acetylhexosamines*. The Journal of biological chemistry **283:**7666-7673.
93. Wang X, Hu G, Zhou J. 2010. *Repression of versican expression by microRNA-143*. The Journal of biological chemistry **285:**23241-23250.
94. Clouet J, Grimandi G, Pot-Vaucel M, Masson M, Fellah HB, Guigand L, Cherel Y, Bord E, Rannou F, Weiss P, Guicheux J, Vinatier C. 2009. *Identification of phenotypic discriminating markers for intervertebral disc cells and articular chondrocytes*. Rheumatology **48:**1447-1450.
95. Wang LW, Leonhard-Melief C, Haltiwanger RS, Apte SS. 2009. *Post-translational modification of thrombospondin type-1 repeats in ADAMTS-like 1/punctin-1 by C-mannosylation of tryptophan*. The Journal of biological chemistry **284:**30004-30015.
96. Stanton H, Melrose J, Little CB, Fosang AJ. 2011. *Proteoglycan degradation by the ADAMTS family of proteinases*. Biochimica et biophysica acta **1812:**1616-1629.
97. Dranoff JA, Bhatia N, Fausther M, Lavoie EG, Granell S, Baldini G, Hickman DA, Sheung N. 2013. *Posttranslational regulation of tissue inhibitor of metalloproteinase-1 by calcium-dependent vesicular exocytosis*. Physiological reports **1:**e00125.
98. Scilabra SD, Troeberg L, Yamamoto K, Emonard H, Thogersen I, Enghild JJ, Strickland DK, Nagase H. 2013. *Differential regulation of extracellular tissue inhibitor of*

86

metalloproteinases-3 levels by cell membrane-bound and shed low density lipoprotein receptor-related protein 1. The Journal of biological chemistry **288:**332-342.

99. Freund A, Orjalo AV, Desprez PY, Campisi J. 2010. *Inflammatory networks during cellular senescence: causes and consequences.* Trends in molecular medicine **16:**238-246.

100. Stetler-Stevenson WG. 2008. *The tumor microenvironment: regulation by MMP-independent effects of tissue inhibitor of metalloproteinases-2.* Cancer metastasis reviews **27:**57-66.

101. Murphy G. 2011. *Tissue inhibitors of metalloproteinases.* Genome biology **12:**233.

102. Yurube T, Takada T, Suzuki T, Kakutani K, Maeno K, Doita M, Kurosaka M, Nishida K. 2012. *Rat tail static compression model mimics extracellular matrix metabolic imbalances of matrix metalloproteinases, aggrecanases, and tissue inhibitors of metalloproteinases in intervertebral disc degeneration.* Arthritis research & therapy **14:**R51.

103. Vo NV, Hartman RA, Yurube T, Jacobs LJ, Sowa GA, Kang JD. 2013. *Expression and regulation of metalloproteinases and their inhibitors in intervertebral disc aging and degeneration.* The spine journal : official journal of the North American Spine Society **13:**331-341.

104. Rajagopalan S, Meng XP, Ramasamy S, Harrison DG, Galis ZS. 1996. *Reactive oxygen species produced by macrophage-derived foam cells regulate the activity of vascular matrix metalloproteinases in vitro. Implications for atherosclerotic plaque stability.* The Journal of clinical investigation **98:**2572-2579.

105. Deem TL, Cook-Mills JM. 2004. *Vascular cell adhesion molecule 1 (VCAM-1) activation of endothelial cell matrix metalloproteinases: role of reactive oxygen species.* Blood **104:**2385-2393.

106. Moon SK, Kang SK, Kim CH. 2006. *Reactive oxygen species mediates disialoganglioside GD3-induced inhibition of ERK1/2 and matrix metalloproteinase-9 expression in vascular smooth muscle cells.* FASEB journal : official publication of the Federation of American Societies for Experimental Biology **20:**1387-1395.

107. Cook-Mills JM. 2006. *Hydrogen peroxide activation of endothelial cell-associated MMPs during VCAM-1-dependent leukocyte migration.* Cellular and molecular biology **52:**8-16.

108. Taganov KD, Boldin MP, Chang KJ, Baltimore D. 2006. *NF-kappaB-dependent induction of microRNA miR-146, an inhibitor targeted to signaling proteins of innate immune responses.* Proceedings of the National Academy of Sciences of the United States of America **103:**12481-12486.

109. Hollander AP. 2010. *Collagen degradation assays.* Methods in molecular biology **622:**367-378.

110. Billinghurst RC, Ionescu M, Poole AR. 2001. *Immunoassay for collagenase-mediated cleavage of types I and II collagens.* Methods in molecular biology **151:**457-472.

111. Roughley PJ, Alini M, Antoniou J. 2002. *The role of proteoglycans in aging, degeneration and repair of the intervertebral disc.* Biochemical Society transactions **30:**869-874.